Evolution of the Chos Malal and Agrio fold and thrust belts, Andes of Neuquén: Insights from structural analysis and apatite fission track dating

E.A. Rojas Vera, J. Mescua, A. Folguera, T.P. Becker, L. Sagripanti, L. Fennell, D. Orts, V.A. Ramos

PII: S0895-9811(15)30067-5

DOI: 10.1016/j.jsames.2015.10.001

Reference: SAMES 1467

To appear in: *Journal of South American Earth Sciences*

Received Date: 31 March 2015

Revised Date: 22 September 2015

Accepted Date: 2 October 2015

Please cite this article as: Rojas Vera, E.A., Mescua, J., Folguera, A., Becker, T.P., Sagripanti, L., Fennell, L., Orts, D., Ramos, V.A., Evolution of the Chos Malal and Agrio fold and thrust belts, Andes of Neuquén: Insights from structural analysis and apatite fission track dating, *Journal of South American Earth Sciences* (2015), doi: 10.1016/j.jsames.2015.10.001.

Evolution of the Chos Malal and Agrio fold and thrust belts, Andes of Neuquén: Insights from structural analysis and apatite fission track dating

Rojas Vera, E.A.[1], Mescua, J.[2], Folguera, A.[1], Becker, T. P.[3], Sagripanti, L.[1], Fennell, L.[1], Orts, D.[1], Ramos V.A.[1]

1) Instituto de Estudios Andinos Don Pablo Groeber (Universidad de Buenos Aires – CONICET).

2) IANIGLA (CONICET) Mendoza.

3) Exxon Mobil Upstream Research Company

Abstract

The Chos Malal and Agrio fold and thrust belts are located in the western part of the Neuquén basin, an Andean retroarc basin of central-western Argentina. Both belts show evidence of tectonic inversion at the western part during Late Cretaceous times. The eastern part is dominated by late Miocene deformation which also partially reactivated the western structures. This work focuses on the study of the regional structure and the deformational event that shaped the relief of this part of the Andes. Based on new field work and structural data and previously published works a detailed map of the central part of the Neuquén basin is presented. Three regional structural cross sections were surveyed and balanced using the 2d Move^{TM} software. In order to define a more accurate uplift history, new apatite fission track analyses were carried on selected structures. These data was used for new thermal history modeling of the inner part of the Agrio and Chos Malal fold and thrust belts. The results of the fission track analyses improve the knowledge of how these fold and thrust belts have grown trough time. Two main deformational events are defined in Late Cretaceous to Paleocene and Late Miocene times. Based on this regional structural analysis and the fission track data the precise location of the orogenic front for the Late Cretaceous-Paleocene times is reconstructed and it is proposed a structural evolution of this segment of the Andes. This new exhumation data show how the Late Cretaceous to Paleocene event was a continuous and uninterrupted deformational event.

Keywords: Andean uplift, exhumation, foreland basin, synorogenic deposits, thin-skinned belt, thick-skinned belt, tectonic inversion.

Introduction

The study area is located at the transition zone between the Southern Central Andes and the Northern Patagonian Andes (Figure 1) (Ramos, 1999). This transition zone coincides at depth with a change in the subduction angle (Pesicek et al., 2012). The Agrio and Chos Malal fold and thrust belts are developed between 36 and 39ºS in the western part of the Neuquén basin, an important petroleum basin of Argentina. At these latitudes the orogen is the product of a normal subduction system between the Nazca plate and the South American plate. Since 26 Ma ago, the Nazca plate is subducted beneath the South American plate (Pardo Casas and Molnar, 1987; Somoza, 1998) with an east dipping angle of 30º and convergence rate of about 7.9 cm/yr (Kendrick et al., 1999) with an oblique convergence vector of 79ºN.

The main features of the Andes at these latitudes are in Chile the Coastal Cordillera, the Central Valley, the present arc and the western part of the main Andes. In Argentina the Andes are formed by the Guañacos, Malargüe, Chos-Malal and Agrio fold and thrust belts developed in the eastern main Andes (Figure 1). A moderated relief of the Pliocene to Quaternary volcanoes reaching 2500 m a.s.l. characterizes this particular segment of the Andes. The Andean uplift starts at about 110-90 Ma ago when the South Atlantic Ocean starts opening (Godoy et al., 1999; Jordan et al., 2001; Charrier et al., 2002; Oncken et al., 2006; Glodny et al., 2007).

The Andes in Chile at these latitudes have limited and isolated outcrops of the Neuquén basin, and the present volcanic arc was developed on the Cura Mallín basin deposits. This basin is characterized by late Oligocene-early Miocene volcanic and continental units, developed in an intra-arc extensional setting presently located in the drainage divide area between Argentina and Chile.

On the Argentinean side the Neuquén Basin is well exposed with a continuous geological record from Triassic to Quaternary times. The basin begun with Jurassic synrift deposits, and continued with a series of Jurassic-Cretaceous marine transgressions and regressions deposited in a retroarc setting with more than 8 km fill (Rojas Vera et al., 2010). The first compressional pulse started building the Andes by Late Cretaceous times, through the inversion of the previously extensional structures. This segment at the western most part is again affected by extension in late Oligocene–early Miocene times, but out of the study area.

A late Miocene compressional event affected both sides of the Andes and was the responsible for final shaping the thin-skinned fold and thrust belts. The Guañacos thick-skinned fold and thrust belt (Figure 1) defined by Folguera et al. (2004) deforms late Oligo-Miocene sequences that accommodates high amounts of compression and is located at the drainage divide area of the main Andes. The Agrio, Chos Malal and Malargüe fold and thrust belts defined by Ramos (1978) are located further east in Argentina (Figure 1) and have a mixed style of deformation. These belts have a western part, immediately to the east of the Guañacos fold and thrust belt, characterized by the presence of thick–skinned structures product of tectonic inversion, and an eastern part dominated by thin-skinned structures.

The aim of this work is focused on how these Andean structures have worked through time; how the tectonic evolution affected the style of deformation, and when these fold belts have been formed. A series of regional balanced structural cross sections has been made through the Agrio and Chos Malal fold and thrust belts to illustrate this evolution, and apatite fission-track analyses were obtained on selected structures. The new data is integrated with the FT data obtained on the western slope of the main Andes at these latitudes (Gräfe et al., 2002, Glodny et al., 2007, and Spiking et al., 2008). This study as a whole presents a better understanding about how these fold and thrust belts were constructed trough time.

Geological setting

The study includes the western part of the Neuquén Basin, as part of the Agrio, Chos Malal and Malargüe fold and thrust belts. The study area shows a relatively geological complexity with Late Paleozoic to Quaternary units. A pre-Jurassic basement is exposed in the central part of the study area in the Cordillera del Viento. This consists in the

Andacollo Group (Hervé et al., 2013) with 2,700 m of Carboniferous marine shales and ignimbrites highly deformed by the Gondwanian orogeny, unconformably covered by 2,000 m of Permian to Triassic volcanic and sedimentary rocks of the Choiyoi Group (Stipanicic, 1968, Ramos et al., 2011). Over these volcaniclastic rocks, also gathered as the pre-Jurassic basement (Figure 2), the pre-Cuyo unit was deposited (Gulisano, 1981), with a highly variable thickness (50 m to 3,000 m), consisting mostly in non marine sediments and volcaniclastic sequences of Late Triassic to Early Jurassic age. These volcaniclastic packages show synextensional geometries in seismic lines (Gulisano and Gutiérrez Pleimling, 1995, Sagripanti et al., 2015).

These sequences have been related to the synrift stage of the Neuquén Basin. A Pacific-derived transgression has led to the deposition of Early Jurassic sequences, corresponding to the Cuyo Group, presently exposed at the eastern slope of the Andes and more locally at its western slope (Gulisano, 1981; Suárez and Emparan, 1997). These deposits covered previous units in a variety of facies from distal offshore shales, turbidites and platform sandstones to distal fluvial facies. These rocks are restricted in the surface to the western sector of the study area, flanking the eastern Loncopué trough, and a narrow belt to the northeast along the orogenic front (Figure 2). At least part of these sequences shows an extensional control similar to the underlying volcaniclastic packages (Vergani et al., 1995). Highly variable thicknesses are also related to these strata as seen in borehole data, being more than 1,500 m thick in the western Agrio fold and thrust belt east of the Loncopué trough (Figure 3). Middle to Late Jurassic sequences (Figure 2) are represented by the transgressive Lotena Group (Legarreta and Gulisano, 1989) and the lower part of the Mendoza Group. The two units are separated by an important marine regression associated with 800 to 10 m thick evaporitic beds and reddish sandstones. These Middle to Late Jurassic transgressive/regressive successions outcrop in the western part of the Agrio and Chos Malal fold and thrust belts and in the orogenic front area to the east (La Yesera anticline) (Figure 2). Over these, a second Pacific transgression covered almost the entire Neuquén Basin in Latest Jurassic to Early Cretaceous times, whose base is the Vaca Muerta Formation (Tithonian-Early Valanginian) with 1,400 m of shales and limestones (Legarreta and Gulisano, 1989). After this, sandstones, shales and limestones indicate a rapid regression followed by another Pacific transgression represented by the Agrio Formation (Valanginian-Early Barremian). Over these rocks, a regressive event, which corresponds to the last incursion from the Pacific Ocean in the area, is marked by the Huitrin Formation (Late Barremian-Aptian) evaporates followed by reddish fluvial and lacustrine Rayoso Formation (Aptian-Albian). A regional angular unconformity separates these beds from the overlying Neuquén Group, whose base was dated at ~ 99 Ma (Tunik et al., 2010). This group is composed by 1,500 m of continental deposits, sandstones, shales and minor conglomerates, unconformably overlying previous Mesozoic units, with the more proximal facies close to the western margin of the basin. It has been interpreted as the foreland basin deposits that records the first Andean exhumation in the region related to orogenic uplift by Tunik et al. (2010), among others. Partly coeval granitoids are cropping out over the western slope of the Andes corresponding to the contemporaneous volcanic arc (out of the study area) (Munizaga et al., 1988; Suárez and Emparan, 1997). Campanian to Maastrichtian Malargüe Group indicates an Atlantic transgression in the foredeep of the Andes at these latitudes that did not cover its western slope beyond the longitude of the Tromen volcanic plateau (Figure 2) (Barrio, 1990; Agruirre Urreta et al., 2010). Coeval volcanic and intrusive rocks are widespread over the eastern slope of the Andes (Figure 3) east of the Loncopué trough (Groeber, 1956; Zöllner and Amos, 1973; Rapela and Llambías, 1985; Llambías and Rapela, 1989; Zamora Valcarce et al., 2006). Older pulses in this magmatic suite correspond to within-plate basaltic to andesitic dykes of 91,97 ± 4,06 Ma (Zamora Valcarce et al., 2006) that are cutting contractional structures at the western Agrio fold and thrust belt (Figure 2), which confirms a Late Cretaceous deformation in the area. A later volcanic pulse is represented by arc related andesitic flows and subvolcanic rocks of 73 to 65 Ma (Figure 2) (Zamora Valcarce et al., 2006). This age zonation has been interpreted as a Late Cretaceous to Paleocene arc expansion at these latitudes (Ramos and Folguera, 2005). The younger part of this group is represented by Eocene andesitic flows at the western Agrio fold and thrust belt (Llambías and Rapela, 1989).

Oligocene to Miocene units are combined in a single group in Figure 2. This includes highly heterogeneous lithologies from the Cura Mallín, Palaoco, Cajón Negro, Mitrauquén, and Tralalhué to Puesto Burgos Formations (Pesce, 1981; Ramos and

Barbieri, 1989; Suárez and Emparán, 1997; Kay et al., 2006; Zamora Valcarce et al., 2006). The late Oligocene to Miocene units are volcanic and clastic successions with highly contrasting lithologies (Figure 3). The oldest volcaniclastic depocenters in the area correspond to the Cura Mallín Basin (González-Ferrán and Vergara, 1962; Niemeyer and Muñoz, 1983) that is developed on both sides of the Andes surrounding the drainage divide between 36º and 39ºS. This succession is highly variable in thickness, with a maximum of 2,000 m. The base has been dated in 25 Ma based on geochronological and biostratigraphic grounds (Sarris 1964; Leanza et al., 2002; Croft et al. 2003; Vergara et al., 1997 b; Suárez and Emparán, 1997; Jordan et al., 2001; Burns, 2002), being divided in the volcaniclastic Río Queuco Member, and the overlying siliciclastic and carbonatic Malla Malla Member (Niemeyer and Muñoz, 1983). These packages have been related to synextensional depocenters between 36º and 39ºS (Jordan et al., 2001; Radic, 2002; Rojas Vera et al., 2010). Over the orogenic front in the eastern side of the Andes (Figure 2), coeval volcanic rocks whose ages are bracketed between 27 and 19 Ma were combined in the Palaoco and Cerrillos Formations (Ramos and Barbieri, 1989; Cobbold and Rossello, 2003; Kay et al., 2006). These have been interpreted as intraplate series erupted in an extensional retroarc region (Ramos and Barbieri, 1989; Kay et al., 2006).

A relatively younger succession corresponding to the Trapa Trapa, Charilehue and Cajón Negro Formations are included in the same group. This sequence has a late Miocene age with a maximum thickness of 1,500 m. It is composed of ignimbrites, lava flows and minor interfingered siliciclastic sequences (Pesce, 1981; Uliana, 1978; Niemeyer and Muñoz, 1983; Utgé et al., 2009). These deposits are exposed from the drainage divide area up to the far-eastern side of the Andes. Both units are deposited over an angular unconformity with Mesozoic to Paleocene strata, implying a mountain building episode during late Early Miocene times. Moreover, they have been interpreted as an eastward expanded arc developed in late Miocene times, presumably linked to a shallowing subduction episode restricted to the north of 37º 40´S (Kay et al., 2006, Spagnuolo et al., 2012). At that time, pyroclastic and clastic successions, up to the latest Miocene, interpreted as coeval synorogenic deposits, were accumulated on both sides of the Andes as the Mitrauquén, Tralalhué and Puesto Burgos Formations (Suárez and Emparán, 1997;

Ramos, 1998; Repol et al., 2002; Leanza and Hugo, 2001; Melnick et al., 2006; Zamora Valcarce et al., 2006).

Pliocene to Quaternary volcanic rocks were erupted from the arc zone in the drainage divide area to the retroarc zone in the Tromen volcanic plateau area (Figure 2). Pliocene rocks of the Cola de Zorro Formation have a maximum thickness of 2,000 m (Vergara and Muñoz, 1982). Quaternary rocks are in the retroarc Tromen volcanic plateau, the Loncopué trough infill and the arc Andean Plateau (Kay et al., 2006; Galland et al., 2007). These units are the expression of the present magmatic arc and coeval retroarc volcanic products during Quaternary times (Stern, 1989; Lara et al., 2001; Varekamp et al., 2010). Pliocene to Quaternary volcanics show synextensional unconformities hosted in extensional depocenters (Folguera et al., 2006; Melnick et al., 2006; Rojas Vera et al., 2010). However, there is local evidence of contraction as discussed by Galland et al. (2007), Messager et al. (2010), and Sagripanti el al. (2015).

Regional structure

The regional structural transect depicted in Figure 3 shows how the different basins blends each other across the entire orogen. This transect integrates structures of the main Andes and the foreland fold and thrust belts. The western slope of the Andes is based on Radic (2010) and the eastern part on Zamora Valcarce (2007a). This section cuts through the Agrio fold and thrust belt (Figure 2). Structures located in the Loncopué trough are based on our field data and gravimetric studies shown in Rojas Vera et al. (2010, 2014). The decollement level was located at 15-24 km depth, dipping 5-3ºW following Zapata et al. (1999) and Zamora Valcarce et al. (2006). This section shows deformation on three partially overlapping basins: 1) the Mesozoic Neuquén Basin exhumed mostly to the east in the Agrio fold and thrust belt; 2) the Oligocene to Miocene Cura Mallín Basin; and 3) thick sequences of Pliocene to Quaternary strata in the Loncopué trough and other sectors of the main Andes. Over the western slope, Jurassic sequences of the Nacientes del Bío Bío Formation are exposed, which are equivalent to those of the western part of the Agrio fold and thrust belt (Suárez and Emparán, 1997). Therefore, gravimetric models include

Early Jurassic sedimentary successions in the retroarc area precisely at the Loncopué trough, beneath thick packages of Cenozoic to Quaternary volcaniclastic rocks (Rojas Vera et al., 2010). One of the particularities of this section is the presence of a long wavelength anticline denominating the Chihuidos High at the orogenic front area, interpreted in this work as a mild tectonic inversion feature of Late Triassic faults following Zamora Valcarce et al. (2006) and Mosquera and Ramos´ (2006) interpretations. Immediately to the west of the Chihuidos High, across the 38ºS transect, the Agrio fold and thrust belt is developed. Most of the structures constitutes an east-vergent imbricate fan interrupted locally by backthrusts. In this transect the eastern Loncopué trough is controlled by a west-dipping Quaternary normal fault. We modeled the Loncopué trough as an inverted graben filled by Mesozoic to Quaternary strata, constrained by seismic, magnetic, and gravity data (Rojas Vera et al., 2014). To the west an imbricate fan of inverted basement east-dipping normal faults is developed in the main Andes. The restoration resulted in a total shortening of 11 km which is equivalent to 4.78 % of the initial length, which is lower than the obtained shortening by Turienzo et al. (2014) further north.

Methods

Structural cross sections

Part of this study was the construction of three structural transects over the Agrio, Chos Malal and Malargüe fold and thrust belts (Figure 4). Using previously published data from Zamora Valcarce et al. (2007a), Rojas Vera et al. (2010), and field data obtained by the authors. Main new observations were conducted in Cordillera del Viento, Sierra de Huantraico, the Yesera Anticline, Cerro Rayoso, and many other areas, which were combined with previous field dataset obtained from the 1: 50,000 scale mapping done by part of the authors along the main corridors where the regional sections have been constructed.

Using Midland Valley's software 2DMove^{TM} we were able to construct three regional structural cross sections. These sections were restored, using different algorithms of the 2DMove obtaining their respective shortening rates for each one. The importance of these regional balanced structural sections, which have been benefited with new geological field data, is that allows a more realistic restoration of the undeformed section to illustrate the final evolution of the regional structure.

Apatite fission track

Apatite fission track (AFT) dating was carried out on four samples of Jurassic and Early Cretaceous units from the inner sector of the Agrio fold thrust belt and five samples of Early to Late Cretaceous units from the outer sector of the Chos Malal fold thrust belt. This study is located just south of the fission track analyses made by Folguera et al. (2015) in the Malargüe fold and thrust belt in southern Mendoza region, which is in north of our sampled area.

Sample locations and depositional ages are indicated in Table 1 and Figure 2. These were dated using the external detector method (Tagami and O'Sullivan, 2005) by Geotrack Inc. Ages for 20-22 apatite grains were obtained per sample, except for sample GC 1132-8 where only 10 grains could be dated. Between 46 and 101 track lengths were measured per sample, except for GC 1132-8 (9 tracks) and GC 1132-10 (21 tracks), including angle to c-axis. Chlorine content, the main control for fission track annealing kinematics (Carlson et al., 1999; Barbarand et al., 2003) was also determined.

Thermal history modeling was made using HeFTy (Ketcham, 2005). For this, we analyzed the AFT results for each sample, taking into account the presence of one or more age populations based on the χ^2 test. Samples that fail the χ^2 contain more than one AFT age population due to permanence in the partial annealing zone and different apatite compositions, resulting in a mix of track retention behaviors (Reiners and Brandon, 2006). For thermal history modeling in HeFTy, we only used samples that pass the χ^2 test, indicating a single population of AFT ages. For each of these samples, HeFTy models without restrictions and with restrictions based on geologic information (i.e. prescribing exhumation events according to known deformation ages) were carried out. For each model, 50.000 paths were tried at random using inverse Montecarlo modeling. Each path was evaluated with the “goodness of fit” statistics incorporated in HeFTy, that use the Kolmogorov-Smirnov test with merit values of 0.5 and 0.05 for good and acceptable fits, respectively (Ketcham, 2005).

Structure of the study area

The Agrio fold and thrust belt as defined by Ramos (1978) developed between the Loncopué trough and the Chihuidos high, and is related to Late Cretaceous and late Miocene contractional stages.

The Agrio fold and thrust belt has two domains clearly distinguished by Ramos (1998), Zapata et al. (1999) and Zamora Valcarce et al. (2006). An inner Agrio fold and thrust belt is formed by inverted Triassic to Jurassic half-graben structures that generated long wavelength (up to 10 km) east vergent antiforms. The outer Agrio fold and thrust belt shows the development of thin-skinned structures detached from Late Jurassic evaporites and shales, where shortening is transferred from the western basement blocks to the east, beneath the inner sector. Most of the structures constitute an east vergent imbricate fan locally interrupted by backthrusts.

One of the particularities of this area is the presence at the orogenic front area of a long wavelength antiformal structure, the Chihuidos High. Even though a flexural origin has been proposed for the Chihuidos (Sigismondi and Ramos, 2008), we follow interpretations in which this high is the result of tectonic inversion (Mosquera and Ramos, 2006; Zamora Valcarce et al., 2006).

For the present work we selected three regional cross-sections for the structural transects which are depicted in figures 2 and 4.

We summarized in figure 4 the three transects, to show how the structure changes from north to south. The most important change between sections is observed in the northernmost transect. The western structures are dominated by the Chos Malal fold and thrust belt, while those located to the east are part of the Malargüe fold and thrust belt.

Cordillera del Viento - Huantraico section

The structural section is composed, from west to east, by the Cordillera del Viento block, the Chos-Malal fold and thrust belt, the Tromen volcanic plateau, the Malargüe fold and thrust belt and the Huantraico frontal syncline.

The Cordillera del Viento is an east vergent basement block with a wavelength of more than 20 km. This structure is one of the few places where the Paleozoic/Triassic basement of the basin is exposed in the Neuquén Basin. The main fault system is located to the east of the Cordillera del Viento. Two anticlines are located next to this structure near Cerro la Parva (Figures 2 and 5) of short wave length (2-3 km). They have east vergence and are structurally related to the Cordillera del Viento block (see also detail structures depicted by Sanchez et al., 2014, 2015). These structures seem to be detached at the Auquilco Formation (Oxfordian-Kimmeridgian), which is one of the important detachment levels of the basin. The basement structures, when inverted, deform the upper levels constituted by shales and gypsum units of the Auquilco, Vaca Muerta, Agrio, and Hutrín Formations, producing smaller wave length structures associated with a shallower detachment. Basement shortening is then transferred to upper levels deforming the sedimentary cover, accommodating shortening, and developing the thin-skinned structures.

Immediately to the east, the anticlines of Río Curelieuvú and Arroyo Blanco are developed with opposite vergence. Their geometry at surface (Figure 5) is related to a west-vergent basement structure that forms a triangle zone in the Chos Malal fold and thrust belt. Some authors proposed a more complex basement structure (see Turienzo et al. 2014, and Sánchez et al., 2014, 2015).

The double vergent basement block of Tromen is forming the Arroyo Blanco anticline to the west, and the east-vergent structure of La Yesera anticline. This structure is characterized by the anomalous thicknesses of gypsum of the Auquilco Formation. Zapata et al. (1999) and Zamora Valcarce et al. (2006) suggest salt migration of Auquilco Formation evaporates into the crest of some structures.

Immediately to the east, the Pampa Tril anticline and the Huantraico syncline are located, which are related to a triangle zone, where the Huantraico syncline is the frontal monocline of these structures.

Pampa Tril Anticline is composed by two minor structures: Laguna Auquilco syncline and Filo Morado anticline, both structures have east-vergence. To the east of the Huantraico frontal syncline a series of backthrusts develops out of the section.

This triangle zone has being recognized as the Miocene orogenic front of the basin. The structure in this cross-section is simplified from a more detailed model proposed by Zamora Valcarce et al. (2006).

The easternmost structure of this transect is composed by the Chihuido de la Salina anticline. This domal structure is formed by intrusion of magmatic rocks at different levels.

The performed restoration of this regional section shows a total shortening of 9.5 kilometers at these latitudes.

Naunauco- Loma Rayoso section

The second cross-section is located in the Agrio fold and thrust belt (Figure 6). Regional structure is the result of a combination of thin- and thick-skinned structures. Over the western part of the section the Cholar Anticline is developed (Figure 6). It is an east vergent basement structure, with a wavelength of more than 12 kilometers, similar but lower than the one depicted in Cordillera del Viento. The main difference between these basement structures is the level of exhumation. The basement in Cordillera del Viento is exposed at 2,991 m a.s.l. (Choiyoi Group), whereas to the south Late Jurassic units are present at surface, such as the Vaca Muerta Formation, being the top of the basement at least at 2,000 m depth.

Immediately to the east, the presence of a backthrust is defining a triangle zone, which shows the development of a minor structure. A series of east-vergent anticlines at the Cerro Naunauco area are detached in Auquilco Formation. In fact, a series of anticlines are formed between Cerro Naunauco and Loma Rayoso anticlines by the same mechanism, but with opposite vergence. The characteristics of the decollment level are described by Zamora Valcarce et al. (2006) and Rojas Vera et al. (2014), based on seismic lines located immediately to the south. The lines show how basement structures are transferring displacements at shallower levels. This mechanism is very effective to transfer shortening to the foreland as shown by Kozlowski et al. (1998). The last detached structure is Loma Rayoso anticline, where the fault is inserted at Bajada del Agrio Group forming a backthrust. The Chihuidos high to the east of the triangle zone is the result of tectonic inversion that produced these long wavelength structures. Cerro Villegas syncline is a very large frontal structure where Miocene volcanic rocks are exposed along the axial part. Chihuido Oeste anticline, immediately to the east of the Chihuido del Medio anticline and Chihuido Este anticline (Ramos, 1981) are interpreted as inverted basement structures where Late Cretaceous synorogenic sequences are folded. Restoration of the section indicates a 9.6 km of shortening.

Cerro Mocho Section

This section starts with Mulichinco and Cerro Mocho anticlines in the western side (Figure 7). Mulichinco Anticline is an east vergent basement structure with a relative high level of exhumation where Early Jurassic sequences of the Cuyo Group are exposed. Another basement structure, the Cerro Mocho Anticline, is developed to the east. It is interpreted as a doubly vergent basement structure with a wavelength larger than 10 km. Outcrops of Vaca Muerta Formation at Cero Mocho have the best level of exposure in the entire basin, after Sierra de la Vaca Muerta located south of the Las Lajas town. This area also contains the westernmost well drilled on the entire basin. This well registered more than 1,000 meters of Molles Formation. The next structure to the east is Pichaihue Anticline, which based on its west-vergence, was interpreted as the result of a basement backthrust. Pampa del Salado syncline is surrounded by the Pichaihue anticline to the west and Salado anticline to the east.

The complex structural geometry of Salado and Pichi Mula anticlines was described by Zapata et al. (1999) and Zamora Valcarce et al. (2006), based on well and seismic data of Y.P.F. S.A. These structures are detached at shallower levels in the Auquilco Formation forming anticlines of 2-4 kilometers wavelength. At surface Pichi Mula anticline is overthrust on top of the Salado anticline. To the west, a series of east-vergent basement structures are developed. The structure of the Chihuidos High is composed by Chihuido Oeste and Chiuido del Medio anticlines, where Bajada del Agrio Group is exposed in the axial part of the anticlines, while in the syncline axes the Neuquén Group outcrops. A shortening of 9 km was obtained by the palinspastic restoration.

AFT results and thermal history modelling

The results of fission track ages and lengths are presented in Table 2. Even though most samples have AFT ages younger than their depositional age, only three of them pass the χ^2 test.

The seven remaining samples contain more than one population of AFT ages. This can be explained as a result of partial resetting of the AFT system, indicating (a) that the ages are detrital and therefore populations reflect different sediment sources, (b) that variations in apatite composition produce different annealing rates and the observed spread in ages, (c) a combination of both.

For the second case, according to Barbarand et al. (2003) chlorine content is the main compositional control on AFT ages for apatites with Cl >0.35 wt%, with Cl-rich apatites being more resistant to annealing, and having therefore older ages. All samples that fail the χ^2 test contain apatites with Cl >0.35 wt%, in spite of which a relationship of increase in age with chlorine content is not observed in any case. Therefore, we interpret the presence of more than one population of AFT ages as the result of partial annealing of apatites from different sediment sources. This is supported for samples GC1132-2, GC1132-4 and GC1132-6 by the presence of pre-depositional ages. A study of the detrital ages exceeds the aims of this work, and would need a knowledge of AFT ages in the source regions that is not currently available. In the case of samples GC1132-1, GC1132-3 and GC1132-7, all ages are younger than depositional. We interpret that apatites in these samples were partially annealed, and only a few grains (if any) were completely reset. We conclude that those seven samples were never heated to temperatures higher than the base of the partial annealing zone for apatite fission tracks (~125ºC for apatites of average composition, Reiners and Brandon, 2006).

For the three samples that do not fail the χ^2 test (GC 1132-5, 8 and 10) we used HeFTy to obtain thermal history models (Figure 8).

Sample GC1132-10 corresponds to the oldest unit sampled (Lajas Fm., Bajocian-Bathonian). Thermal history modeling of this sample indicated maximum temperatures between 140ºC and 190ºC during the Early Cretaceous (Figure 8). All models include a major exhumation event around 40 Ma, which left the sample at ~50º-60ºC. A Cretaceous exhumation event (120-80 Ma) is recorded in some models with good fit to the data, although other good models do not require it. Final exhumation of the sample took place since 7 Ma.

Sample GC1132-8, from the Tordillo Formation (Kimmeridgian), provided few datable apatites. Therefore the results of thermal history modeling are not very precise (Figure 8). Best models indicate a Late Cretaceous-Paleogene exhumation event, roughly between 70 and 55 Ma, from maximum temperatures between 140º and 150º to a temperature of ~60ºC. Exhumation to the surface is not well constrained: slow exhumation since 55 Ma, rapid exhumation in the last 10 Ma or intermediate paths all provide good fit to the data.

Sample GC1132-5 corresponds to the Mulichinco Formation (Valanginian), and experienced maximum temperatures between 100º and 160ºC, with best results between 140º and 155ºC (Figure 8). Best models indicate two exhumation stages: a Late Cretaceous to Paleogene event (70-40 Ma) and a Miocene event younger than 10 Ma.

Exhumation and deformational episodes

The results of fission track dating allow us to define an internal sector in which the AFT system was reset, and an external sector in which samples were never buried to the base of the AFT partial annealing zone (Figure 9), indicating a higher amount of exhumation in the internal zone. These sectors coincide with the structural separation of the Agrio fold and thrust belt based on the predominance of basement and cover structures (Ramos, 1998; Zamora Valcarce et al., 2006).

In the internal sector, thermal history models have allowed us to determine two events of exhumation: the first in the late Cretaceous to Paleocene and the second in the Miocene. Cretaceous exhumation can be related to the initial Andean deformation that has been widely documented in the study area (Keidel, 1925; Groeber, 1929; Wichmann, 1934; Ramos, 1981; Zapata et al., 2002; Cobbold and Rossello, 2003; Zamora Valcarce et al., 2006, 2007a, 2009; Tunik et al., 2010). According to Zamora Valcarce et al. (2006, 2007b, 2009), the inversion of Mesozoic normal faults generated the thick-skinned anticlines of the inner sector between 100 and 73 Ma. These faults transferred shortening to the cover using a detachment in Jurassic and Cretaceous evaporites, forming the thin-skinned structures of the outer sector coetaneous with basement deformation in the inner sector.

Best results of thermal history modeling indicate a delay between deformation and exhumation, with the latter beginning around 70 Ma. Similar results have been found by fission track analyses by Folguera et al. (2015) in southern Mendoza in the westernmost part of the Malargüe fold and thrust belt. A protracted history of exhumation reaching well into the Paleogene (55-40 Ma) could also be determined. During this time, the deformation in the outer sector may have taken place in a wedge-top environment without important uplift, and the foreland deposits of the Neuquén Group and younger units deposited over the forming detachment folds. This explains the unreset AFT ages found in this sector. While the latest Cretaceous-early Paleocene exhumation seems related to the late Cretaceous deformation, the exhumation interval, and in particular the 40 Ma exhumation event clearly determined in sample GC1132-10, overlaps the Eocene deformation event proposed by Cobbold and Rosello (2003) for the area. More thermochronological work is needed to determine if this exhumation corresponds to a regional deformation phase or is only local.

Miocene exhumation is recorded in the three modeled samples, although the onset and duration of this event could not be determined from the dataset presented in this work. This event can be related to the compressive deformation that affected all sectors of the fold and thrust belt (Zamora Valcarce et al. 2006, 2009). According to the models presented in this work, high exhumation rates likely started in the region around ~15-10 Ma.

Implications for the thermal gradient in the Neuquén basin

Sample GC1132-7, of the Mulichinco Formation, was partially (not fully) reset for the AFT system. For apatites of average composition, the partial annealing zone extends between 75º and 125ºC (Reiners and Brandon, 2006).

The Neuquén basin rocks preserved at this latitude indicate a sedimentary column of ~2,850 m deposited over the Mulichinco Formation in the Late Cretaceous (Table 3).

Assuming a normal geothermal gradient of 30ºC/km, this sediment thickness would place the sample within the apatite partial annealing zone at 85,5ºC.

Unfortunately, no constrains are available to know if the foreland sediments of the Neuquén Group were deposited in the location of sample GC1132-7.

If we assume that the maximum thickness found for this unit to the east was deposited over this location before the arrival of the Late Cretaceous–Paleogene deformation, assuming again a geothermal gradient of 30ºC/km, the temperature at a depth of 3,850 m would be 115ºC. In this case, a slight increase in the gradient would place the sample below the apatite partial annealing zone, where its apatites would have been reset. This would imply that the thermal gradient was normal during the Late Cretaceous in the area of sample GC1132-7. An increase in gradient in more recent times might have taken place, provided that the sample was already at a shallower depth due to the exhumation related with Late Cretaceous deformation.

In contrast, if no sediments of the Neuquén Group were deposited, a higher gradient is allowed for the Late Cretaceous, since the sample would remain below 125ºC with gradients up to 44ºC/km.

Future works may provide more data to solve this issue.

Unit	Thickness [m]	Total Thickness [m]
Lower Agrio Formation	650	650
Upper Agrio Formation	1400	2050
Rayoso Formation	800	2850
Neuquén Group (?)	1000 (max)	3850

Table 3

Regional shortening variations from north to south across the Neuquén basin

Several publications have proposed that the shortening rates are larger in the northern part of the basin along the flat slab zone. In this sense, Giambiagi et al. (2012) recognize between 33º30` to 36ºS that the amount of shortening decreases significantly. Whereas shortening rates decrease between 34º and 35ºS from 48 km to 20 km; further south between 35º to 36º S shortening decrease from 20 km to 10 km (Turienzo et al. (2014), Sánchez et al. (2015). However, shortening rates stabilize from 37º to 38º in about 10 km, and similar values were obtained between 41º-43ºS by Orts et al. (2015) and Bechis et al. (2014). In a regional analysis we can identify a trend of shortening decrease controlled by the subduction system. While to the north, the development of the flat slab concentrates maximum shortening rates, south of the flat slab zone, only minor variations are present due to crustal and lithospheric structures.

Discussion and concluding remarks

From the thermal history models obtained and the field data analysis we can clearly identify the orogenic front for the Late Cretaceous- Paleocene deformational event (Figure 10). The new FT data show in the southernmost sections how the inner parts of the Agrio fold and thrust belt was uplifted. Similar facts have been identified further north by the FT data of Folguera et al. (2015) in the Malargüe fold and thrust belt, which confirmed previous structural studies in the inner part of the Andes of southern Mendoza (Mescua et al., 2013). The Cordillera de Viento in the northern section was already a high feature constraining the deposition of the latest Cretaceous Malargüe Group, which represents the first Atlantic transgression of the Neuquén Basin (Aguirre Urreta. et al. 2010).

The structural evolution of Cordillera del Viento-Sierra de Huantraico section is summarized in Figure 11. The first uplift was at Cordillera del Viento block at the inner part of the section. The Late Cretaceous exhumation stage at these latitudes was well recognized by several authors (Ramos and Folguera, 2005; Cobbold and Rossello, 2003; Zamora Valcarce et al. 2006). At this time, the magmatic arc starts migrating to the foreland region.

The last exhumation episode occurred in late Miocene (15-10 to 0 Ma)**.** This exhumation stage was previously recognized by several authors based on the age of the synorogenic deposits (Cobbold and Rossello, 2003; Ramos and Folguera, 2005; Zamora Valcarce et al. 2006). Cerro Negro anticline and other structures of west-vergence, which have been interpreted as related to a backthrust beneath La Yesera Anticline, were activated at that time. Pampa Tril anticline as well as the Chihuido de la Salina Negra anticline was also developed at similar times.

Evolution of the Naunauco-Loma Rayoso cross-section (Figure 12) is somewhat different. This particular section was previously analyzed by Zamora Valcarce (2007a) who identified a Late Cretaceous event. This event reflects the development in the western part of the Agrio fold and thrust belt basement structures. This event is also recorded at the inner part of the section (Sample GC1132-5) at El Cholar anticline which is a basement structure like the Cordillera del Viento.

A coeval early Eocene event is well documented in Chile. A recent seismic line obtained in Arauco onshore basin (37º-39º S), shows Eocene deformation according to Becerra et al. (2013). Cobbold and Rossello (2003) also recognized this event at these latitudes on the eastern side of the Andes. This event was not recognized in the thermal history models carried for sample GC1132-5.

The last exhumation event is interpreted as Late Miocene (10 Ma). This event is present in sample GC1132-5 at the inner part of the cross section in the El Cholar anticline. It is also affecting the Loma Rayoso anticline and the Chihuidos High.

The presence of these ages over the entire Agrio fold and thrust belt reveals that the late Miocene event constitutes the most general cooling/exhumation episode occurred in the basin. Loma Rayoso anticline was also uplifted by this age. The stratigraphic record of Cerro Villegas, immediately to the east, indicates that the triangle zone was constructed at this time.

The evolution of the Cerro Mocho section is summarized in Figure 13. A Late Cretaceous- Paleocene event, as it has been previously noted, can be interpreted based on samples GC1132-10 and GC1132-8. These samples are located over Cerro Mocho and Mulichinco anticlines. Both basement structures are placed at the inner part of the Agrio fold and thrust belt. This event again is related to reactivation of basement structures. An exhumation event at 40 Ma determined for sample GC1132-10 may be related to the Eocene deformation proposed by Cobbold and Rossello (2003). However this thermal event was identified in a single sample.

Last exhumation stage is interpreted to be early late Miocene in both samples. Again this exhumation stage is the most broadly recorded in this section, where almost the entire fold and thrust belt was reactivated. The Mulichinco anticline, controlled by basement structures, has been reactivated by an out-of-sequence thrust. An analog situation seems to have occurred in Cerro Mocho Anticline. This final uplift of the Agrio fold and thrust belt is also evidenced by the presence of synorogenic Tralalhue Conglomerates located in piggy-back basins present in the area (Ramos, 1998; Zamora Valcarce et al. 2006). This exhumation event reaches the Chihuidos high structure, where the same exhumation stage was recognized by Zamora Valcarce et al. (2009).

As a summary of the different exhumation episodes it is possible to state that first exhumation took place on the Late Cretaceous to Paleocene. This deformation event (Figure 10) is present in all the studied sections. This particular event is responsible for the uplift of Cordillera del Viento block at the Chos Malal fold and thrust belt and the first detachment developed on the Agrio fold and thrust belt, at the Naunauco-Loma Rayoso area. At the same time tectonic inversion affected the inner part of the Agrio fold and thrust belt at Cerro Mocho and Mulichinco anticlines. This event is confirmed by the presence of the thick synorogenic deposits of the Neuquén Group to the east, and if maturation allowed could be responsible for the potential migration of the oil to the eastern flank of the basin.

The late Miocene exhumation stage in some inner areas beginning in middle Miocene, is well developed after 10 Ma and is the broadest cooling episode represented in the three sections. In the northern section La Yesera anticline was activated at this time. Pampa Trill and Chihuido de la Salina Negra anticlines were uplifted at the same time. To the south in Naunauco-Loma Rayoso section, the reactivation of El Cholar Anticline, Loma Rayoso Anticline and the last exhumation episode of the Chihuidos High took place at this time. The inner part at Cerro Mocho section was also reactivated in the Mulichinco and Cerro Mocho anticlines. The structures at Salado and Pichi Mula anticlines were developed as it is indicated by the presence of synorogenic deposits on piggy-back basins. Contemporaneously, last uplift was registered in the southern and easternmost part of the Chihuidos High, where Zamora Valcarce et al. (2009) obtained similar exhumation ages.

As a final conclusion it is important to remark that the Late Cretaceous uplift was restricted to the western part and that the late Miocene reactivated the western part and also uplifted the eastern sectors. However, the magnitude of both episodes can be evaluated based on the thickness and volume of the synorogenic deposits: while, the Late Cretaceous deformation is associated with more than 1,500 m of synorogenic deposits Miocene deformation is associated with less than 150 m of synorogenic deposits in the Neuquén region. Therefore Late Cretaceous deformation appears as the main orogenic episode of the Andean system at these latitudes.

Acknowledgments

The authors want to recognize the support received by EXXON to obtain the FT data, and the many lively discussion with several members of the *Laboratorio de Tectónica Andina* through the years. We also like to acknowledge Midland Valley Corporation for academic license of the Move^{tm} software. This is the contribution R-177 of the Instituto de Estudios Andinos Don Pablo Groeber.

References

Aguirre-Urreta, B., Tunik, M., Naipauer, M., Pazos, P., Ottone, E., Fanning, M., Ramos, V.A. 2011. Malargüe Group (Maastrichtian–Danian) deposits in the Neuquén Andes, Argentina: Implications for the onset of the first Atlantic transgression related to Western Gondwana break-up. Gondwana Research 19, 482–494.

Barbarand, J., Carter, A., Wood, I., Hurford, T. 2003. Compositional and structural control of fission-track annealing in apatite. Chemical Geology 198, 107-137.

Barrio, C.A. 1990. Late Cretaceous-Early Tertiary sedimentation in a semi-arid foreland basin (Neuquén Basin, Western Argentina). Sedimentary Geology 66, 255–275.

Becerra, J., Contreras-Reyes, E., Arriagada, C. 2013. Seismic structure and tectonics of the southern Arauco Basin, south-central Chile (~38°S). Tectonophysics 592, 53-66.

Bechis, F., Encinas, A., Concheyro, A., Litvak, V. D., Aguirre-Urreta, B., Ramos, V.A. 2014. New age constraints for the Cenozoic marine transgressions of northwestern

Patagonia, Argentina (41°–43° S): Paleogeographic and tectonic implications, Journal of South American Earth Sciences 52, 72-93.

Burns, W.M. 2002. Tectonics of the Southern Andes from stratigraphic, thermochronologic, and geochemical perspectives, PhD thesis (Unpublished), Cornell University, 218 pp., Ithaca.

Carlson, W.D., Donelick, R.A., Ketcham, R.A. 1999. Variability of apatite fission-track annealing kinetics: I. Experimental results. American Mineralogist 84: 1213– 1223.

Charrier, R., Baeza, O., Elgueta, S., Flynn, J., Gans, P., Kay, S., Muñoz, N., Wyss, A., Zurita, E. 2002. Evidence for Cenozoic extensional basin development and tectonic inversion south of the flat-slab segment, southern Central Andes, Chile (33°–36°S.L.). Journal of South American Earth Sciences 15, 117–139.

Cobbold, P., Rossello, E. 2003. Aptian to recent compressional deformation, foothills of the Neuquén Basin, Argentina. Marine and Petroleum Geology 20, 429–443.

Folguera, A., Ramos, V.A., Hermanns, R.L., Naranjo, J., 2004. Neotectonics in the foothills of the southernmost central Andes (37°-38°S): Evidence of strike-slip displacement along the Antiñir-Copahue fault zone. Tectonics 23. Doi: 10.1029/2003TC001533

Folguera, A., Zapata, T., Ramos, V., 2006. Late Cenozoic extension and the evolution of the Neuquén Andes. In: Kay, S.M., Ramos, V.A. (Eds.), Evolution of an Andean Margin: A Tectonic and Magmatic View from the Andes to the Neuquén Basin (35°-39°S Lat.). Geological Society of America, Special Paper 407, 267–285.

Folguera, A., Bottesi, G., Duddy, I., Martín-González, F., Orts, D., Sagripanti, L., Rojas Vera, E. y Ramos, V.A. 2015. Exhumation of the Neuquén Basin in the southern Central Andes (Malargüe fold and thrust belt) from field data and low-temperature thermochronology. Journal of South American Earth Sciences (on line).

Galland, O., Hallot, E., Cobbold, P.R., Ruffet, G., De Bremond d'Ars, J. 2007. Volcanism in a compressional Andean setting: A structural and geochronological study of Tromen volcano (Neuquén province, Argentina). Tectonics 26. Doi :10.1029/2006TC002011.

Glodny, J., Gräfe, K., Echtler, H., Rosenau, M. 2007. Mesozoic to Quaternary continental margin dynamics in South-Central Chile (36–42°S): the apatite and zircon fission track perspective. International Journal of Earth Sciences 97, 1271–1291.

Giambiagi, L., Mescua, J., Bechis, F., Tassara, A., Hoke, G. 2012. Thrust belts of the Southern Central Andes: Along-strike variations in shortening, topography, crustal geometry, and denudation. Geological Society of America Bulletin 124 (7-8), 1339-1351.

Godoy, E., Yañez, G., Vera, E, 1999. Inversion of an Oligocene volcano-tectonic basin and uplifting of its superimposed Miocene magmatic arc in the Chilean Central Andes: first seismic and gravity evidences. Tectonophysics 306, 217–236.

González-Ferrán, O., Vergara, M. 1962. Reconocimiento Geológico de la Cordillera de los Andesentre los paralelos 35º y 38º Latitud Sur. Universidad de Chile, Instituto de Geología, Publicación 24, 119 pp.

Gräfe, K., Glodny, J., Seifert, W., Rosenau, M., Echtler, H. 2002. Apatite fission track thermochronology of granitoids at the South Chilean active continental margin (37°S-42°S): implications for denudation, tectonics and mass transfer since the Cretaceous. 5th International Symposium on Andean Geodynamics, Extended Abstracts, pp. 275-278, Toulouse.

Groeber, P. 1929. Líneas fundamentales de la geología de Neuquén, sur de Mendoza y regiones adyacentes. Ministerio de Agricultura, Dirección General de Minas, Geología e Hidrología, Publicación 58, 1-10.

Groeber, P. 1956. La Serie Andesítica patagónica. Sus relaciones, posición y edad. Revista de la Asociación Geológica Argentina 9, 39-42.

Gulisano, C. 1981. El Ciclo Cuyano en el norte del Neuquén y sur de Mendoza. 8th Congreso Geológico Argentino, Actas 3, 579-592, San Luis.

Gulisano, C.A., Gutiérrez-Pleimling, A.R. 1995. Guía de campo: El Jurásico de la Cuenca Neuquina, b) Provincia de Mendoza. Asociación Geológica Argentina, Serie E, 3, 1-111, Buenos Aires.

Hervé, F., Calderón, M., Fanning, C.M., Pankhurst, R.J., Godoy, E. 2013. Provenance variations in the Late Paleozoic accretionary complex of central Chile as indicated by detrital zircons. Gondwana Research 23(3), 1122-1135.

Jordan, T., Burns, W. Veiga, R. 2001. Extension and basin formation in the southern Andes caused by increased convergence rate: A mid-Cenozoic trigger for the Andes. Tectonics 20, 308–324.

Kay, S., Burns, W., Copeland, P.C., Mancilla, O. 2006. Upper Cretaceous to Holocene magmatism and evidence for transient Miocene shallowing of the Andean subduction zone under the northern Neuquén Basin. In: Kay, S.M., Ramos, V.A. (Eds.), Evolution of an Andean Margin: A Tectonic and Magmatic View from the Andes to the Neuquén Basin (35°-39°S Lat.). Geological Society of America, Special Paper 407, 19–60.

Keidel, J. 1925. Sobre la estructura tectónica de las capas petrolíferas en el oriente del territorio del Neuquén. Ministerio de Agricultura, Dirección General de Minas, Geología e Hidrología, Publicación 8, 1-67.

Kendrick, E.C., Bevis, M., Smalley, R.F., Cifuentes, O., Galban, F. 1999. Current rates of convergence across the central Andes: Estimates from continuous GPS observations. Geophysical Research Letters 26, 541–544.

Ketcham, R. 2005. Forward and Inverse Modeling of Low-Temperature Thermo-chronometry Data. Reviews in Mineralogy & Geochemistry 58, 275-314.

Kozlowski, E., Cruz, C., Sylwan, C., 1998. Modelo exploratorio en la faja corrida de la Cuenca Neuquina, Argentina. Boletín Informaciones Petroleras 55, 4-23.

Lara, L., Rodríguez, C., Moreno, H., Pérez de Arce, C. 2001. Geocronología K-Ar y geoquímica del volcanismo plioceno superior-pleistoceno de los Andes del sur (39-42°S). Revista geológica de Chile 28, 67-90.

Leanza, H.A., Hugo, C.A. 2001. Hoja Geológica Zapala 3969-1, Provincia del Neuquén, Escala 1:250.000. Servicio Geológico y Minero Argentino, Boletín 275, 128 pp., Buenos Aires.

Leanza, H.A., Volkheimer, W., Hugo, C.A., Melendi, D.L., Rovere, E., 2002. Lutitas negras lacustres cercanas al límite Paleógeno-Neógeno en la region noroccidental de la provincia del Neuquén: Evidencias palinológicas, Revista Asociación Geológica Argentina 57, 280-288.

Legarreta, L., Gulisano C.A. 1989. Análisis estratigráfico secuencial de la Cuenca Neuquina (Triásico superior- Terciario). In: Chebli, G. and Spalletti, L. (Eds.) Cuencas Sedimentarias Argentinas, Correlación Geológica Serie 6, 221-243, Tucumán.

Llambías, E. J., Rapela C. W. 1989. Las volcanitas de Collipilli, Neuquén (37°S) y su relación con otras unidades paleógenas de la cordillera. Revista de la Asociación Geológica Argentina 44, 224-236.

Melnick, D., Rosenau, M., Folguera, A., Echtler, H. 2006. Neogene Tectonics of the Western flank of the Neuquén Andes, 37°-39°30´S. In: Kay, S.M., Ramos, V.A. (Eds.), Evolution of an Andean Margin: A Tectonic and Magmatic View from the Andes to the Neuquén Basin (35°-39°S Lat.). Geological Society of America, Special Paper 407, 73–95.

Mescua, J., Giambiagi, L.B., Ramos, V.A. 2013. Late Cretaceous Uplift in the Malargiie fold-and-thrust belt (35°S), southern Central Andes of Argentina and Chile. Andean Geology 40(1), 102-116.

Messager, G., Nivière, B., Martinod, J., Lacan, P., Xavier, J.-P. 2010. Geomorphic evidence for Plio-Quaternary compression in the Andean foothills of the southern Neuquén Basin, Argentina. Tectonics 29, doi: 10.1029/2009TC002609.

Mosquera, A., Ramos, V.A. 2006. Intraplate deformation in the Neuquén Embayment. In: Kay, S.M., Ramos, V.A. (Eds.), Evolution of an Andean Margin: A Tectonic and Magmatic View from the Andes to the Neuquén Basin (35°-39°S Lat). Geological Society of America, Special Paper 407, 97-125.

Munizaga, F., Herve, F., Drake, R., Pankhurst, R.J., Brook, M., Snelling, N. 1988. Geochronology of the Lake Region of south-central Chile (39°–42°S): Preliminary results. Journal of South American Earth Sciences 1, 309–316.

Niemeyer, H., Muñoz, J.1983. Geología de la hoja 57 Laguna de la Laja, Región de Bío Bío, escala 1:250,000, Servicio Nacional de Geología y Minería, Santiago, Chile.

Oncken, O., Hindle, D., Kley, J., Elger, K. 2006. Deformation of the central Andean upper plate system—Facts, fiction, and constraints for plateau models. In: Oncken, O., Chong, G., Franz, G., Giese, P., Götze, H., Ramos, V., Strecker, M., Wigger, P. (Eds.), The Andes-Active Subduction Orogeny, Frontiers in Earth Sciences 1, 7–27.

Orts, D. L., Folguera, A., Giménez, M. Ruiz, F., Rojas Vera, E. A., Lince Klinger, F. 2015. Cenozoic building and deformational processes in the North Patagonian Andes, Journal of Geodynamics 86, 26-41.

Pardo-Casas, F., Molnar, P. 1987. Relative motion of the Nazca (Farallon) and South American Plates since Late Cretaceous time. Tectonics 6, 233–248.

Pesce, A.H. 1981. Estratigrafía de las nacientes del Río Neuquén y Nahueve, provincia del Neuquén, 8th Congreso Geológico Argentino, Actas 3, 439-455, San Luis.

Pesicek, J.D., Engdahl, E.R., Thurber, C.H., DeShon, H.R., Lange, D., 2012. Mantle subducting slab structure in the region of the 2010 M8.8 Maule earthquake (30-40°S), Chile. Geophysical Journal International, 191, 317–324.

Radic, J., Rojas, L., Carpinelli, A., Zurita, E., 2002. Evolución tectónica de la Cuenca Terciaria de Cura Mallín, región cordillerana chileno-argentina (36º 30'–39ºS). 15th Congreso Geológico Argentino, Actas3, 233–241, El Calafate.

Radic, J.P. 2010. Las cuencas cenozoicas y su control en el volcanismo de los complejos Nevados de Chillán y Copahue-Callaqui (Andes del Sur, 36-39ºS). Andean Geology 37 (1), 220-246.

Ramos, V.A. 1978. Estructura. In Geología y Recursos Naturales de la provincia de Neuquén, Neuquén. 7th Congreso Geológico Argentino, Asociación Geológica Argentina, Relatorio 99-118.

Ramos, V.A. 1981. Descripción geológica de la Hoja 33c, Los Chihuidos Norte. Boletín del Servicio Geológico Nacional 182, 103 pp., Buenos Aires.

Ramos, V.A. 1998. Estructura del sector occidental de la faja plegada y corrida del Agrio, cuenca Neuquina, Argentina. 10th Congreso Latinoamericano de Geología (Buenos Aires), Actas 2, 105-110.

Ramos, V.A. 1999. Plate tectonic setting of the Andean Cordillera. Episodes 22(3), 183-190.

Ramos, V.A., Barbieri, M., 1989. El volcanismo Cenozoico de Huantraico: edad y relaciones isotópicas iniciales, provincia del Neuquén. Revista de la Asociación Geológica Argentina 43, 210-223.

Ramos, V.A., Folguera, A. 2005. Tectonic evolution of the Andes of Neuquén: Constraints derived from the magmatic arc and foreland deformation. In: Spalletti L., Veiga, G., Schwarz, E. and Howell J. (Eds.), The Neuquén Basin: A Case Study in Sequence Stratigraphy and Basin Dynamics, Geological Society of London, Special Publication 25, 215–35.

Ramos, V.A., Mosquera, A., Folguera, A., García Morabito, E. 2011. Evolución tectónica de los Andes y del engolfamiento Neuquino adyacente. In: Leanza, H.A., Arregui, C., Carbone, O., Danielli, J.C. and Valles, J. (Eds.), Geología y recursos naturales de la provincia del Neuquén, 18th Congreso Geológico Argentino, Asociación Geológica Argentina, Relatorio 335-348.

Rapela, C., Llambías, E. 1985. La secuencia andesítica terciaria de Andacollo, Neuquén, Argentina, 4th Congreso Geológico Chileno, Actas 4, 458-488, Antofagasta.

Reiners, P., Brandon, M.T. 2006. Using thermochronology to understand orogenic erosion. Annual Reviews of Earth and Planetary Sciences 34: 419-466.

Repol, D., Leanza, H., Sruoga, P., Hugo, C. 2002. Evolución tectónica del Cenozoico de la comarca de Chorriaca, Provincia del Neuquén, Argentina. 15th Congreso Geológico Argentino, Actas 3, 200-205, El Calafate.

Rojas Vera, E.A., Folguera, A., Zamora Valcarce, G., Giménez, M., Ruiz, F., Martínez, P., Bottesi, G., Ramos, V.A., 2010. Neogene to Quaternary extensional reactivation of a fold and thrust belt: The Agrio belt in the Southern Central Andes and its relation to the Loncopué trough (38°–39°S). Tectonophysics 492, 279–294.

Rojas Vera, E.A., Folguera, A., Zamora Valcarce, G., Bottesi, G., Ramos, V.A. 2014. Structure and development of the Andean system between 36-39ºS. Journal of Geodynamics 73, 34-52.

Sagripanti, L., Rojas Vera, E., Gianni, G.M., Folguera, A., Harvey, J.E., Farías, M., Ramos, V.A. 2015. Neotectonic reactivation of the western section of the Malargüe fold and thrust belt (Tromen volcanic plateau, Southern Central Andes). Geomorphology 232, 164–181.

Sánchez, N., Turienzo, M., Dimieri, L., Araujo, V., 2014. Evolución de las estructuras andinas en la faja corrida y plegada de Chos Malal: interacción entre el basamento y la cubierta sedimentaria de la Cuenca Neuquina. Revista Asociación Geológica Argentina 71 (2): 233-246.

Sánchez, N., Turienzo, M., Lebinson, F., Araujo, V., Coutand, I., Dimieri, L. 2015. Structural style of the Chos Malal fold and thrust belt, Neuquén basin, Argentina: Relationship between thick- and thin-skinned tectonics. Journal of South American Earth Sciences (in press).

Sarris, M.,1964. Informe geológico de la zona de Río Palao, Dto. Minas– Provincia de Neuquén. Yacimientos Carboníferos Fiscales, Open File Report 907, 20 pp. Buenos Aires.

Sigismondi, M.E., 2013. Estudio de la deformación litosférica de la cuenca Neuquina: estructura termal, datos de gravedad y sísmica de reflexión. PhD Thesis, Universidad de Buenos Aires (unpublished) 380 p.p. Buenos Aires.

Sigismondi, M., Ramos, V.A., 2008. El flujo de calor de la Cuenca Neuquina. In: Soldo, J., Sigismondi, M. (Eds.), La Geofísica: integradora del conocimiento de subsuelo, Instituto Argentino del Petróleo y el Gas, 55-94.

Somoza, R., 1998. Updated Nazca (Farallon)-South America relative motions during the last 40 My: implications for mountain building in the central Andean region. Journal of South American Earth Sciences 11, 211–215.

Spagnuolo, M.G., Folguera, A., Litvak, V., Rojas Vera E.A., Ramos, V.A. 2012. Late Cretaceous arc expansion in the Southern Central Andes at 36, 5ºS: Evidence for two-episodes of slab shallowing during Andean development. Journal of Geodynamics 38, 44-56.

Spikings, R., Dungan, M., Foeken, J., Carter, A., Page, L., Stuart, F., 2008. Tectonic response of the central Chilean margin (35–38°S) to the collision and subduction of heterogeneous oceanic crust: a thermochronological study. Journal of the Geological Society 165, 941–953.

Stern, C., 1989. Pliocene to present migration of the volcanic front, Andean Southern Volcanic Zone. Andean Geology 16, 145–162.

Stipanicic, P.N., Rodrigo, F., Baulies, O.L., Martínez. C.G. 1968. Las Formaciones presenonianas en el denominado Macizo Nordpatagónico y regiones adyacentes. Revista de la Asociación Geológica Argentina 23(2), 67-98.

Suárez, M., Emparán, C. 1997. Hoja Curacautín 71, Regiones de la Araucanía y del Bío Bío: escala 1:250,000. ed. Servicio Nacional de Geología y Mineria de Chile, 105 pp., Santiago.

Tagami, T., O'Sullivan, P.B. 2005. Fundamentals of fission-track thermochronology. Reviews of Mineralogy and Geochemistry 58, 19-47.

Tunik, M., Folguera, A., Naipauer, M., Pimentel, M., Ramos, V.A., 2010. Early uplift and orogenic deformation in the Neuquén Basin: Constraints on the Andean uplift from U–Pb and Hf isotopic data of detrital zircons. Tectonophysics 489, 258–273.

Turienzo, M., Sánchez, N., Dimieri, L., Lebinson, F., Araujo, V. 2014. Tectonic repetitions of the Early Cretaceous Agrio Formation in the Chos Malal fold-and-thrust belt, Neuquén Basin, Argentina: Geometry, kinematics and structural implications for Andean building. Journal of South American Earth Sciences 53, 1-19.

Uliana, M. 1978. Estratigrafía del Terciario. 7th Congreso Geológico Argentino, Geología y Recursos Naturales del Neuquén, Asociación Geológica Argentina, Relatorio, 67–84.

Utge, S., Folguera, A., Litvak, V., Ramos, V.A. 2009. Geología del sector norte de la cuenca de Cura Mallín: zona de las Lagunas de Epulafquen (36°40′–50′S, 71°–71°10′O). Revista de la Asociación Geológica Argentina 64, 231–248.

Varekamp, J., Hesse, A., Mandeville, C. 2010. Back-arc basalts from the Loncopue graben (Province of Neuquen, Argentina). Journal of Volcanology and Geothermal Research 197, 313–328.

Vergani, G.D., Tankard, A.J., Belotti, H.J., Welsink, H.J. 1995. Tectonic evolution and paleogeography of the Neuquén Basin, Argentina. In: Tankard, A.J., Suárez, R., Welsink, H.J. (Eds.), Petroleum Basins of South America. APPG Memoir 62, 383–402.

Vergara, M., Muñoz, J. 1982. La Formación Cola de Zorro en la Alta Cordillera andina chilena (36^o-39^o Lat. S), sus características petrográficas y petrológicas: una revisión. Revista geológica de Chile 17, 31–46.

Vergara, M., Moraga, J., Zentilli, M. 1997. Evolución termotectónica de la cuenca terciaria entre Parral y Chillán: análisis por trazas de fisión en apatitas. In 8° Congreso Geológico Chileno (Antofagasta), Actas 2, 1574-1578.

Wichmann, R. 1934. Contribución al conocimiento geológico de los territorios del Neuquén y del Río Negro. Ministerio de Agricultura, Dirección General de Minas y Geología, Boletín 39, 1-27.

Zamora Valcarce, G., Zapata, T., Del Pino, D., Ansa, A. 2006. Structural evolution and magmatic characteristics of the Agrio fold-and-thrust belt. In: Kay, S.M., Ramos, V.A. (Eds.), Evolution of an Andean Margin: A Tectonic and Magmatic View from the Andes to the Neuquén Basin (35°-39°S Lat), Geological Society of America, Special Paper 407, 125–145.

Zamora Valcarce, G. 2007a. Estructura y Cinemática de la faja plegada y corrida del Agrio,Cuenca Neuquina. PhD Thesis, Universidad de Buenos Aires (unpublished) pp. 303, Buenos Aires,

Zamora Valcarce, G., Rapalini, A.E., Spagnuolo,C.M. 2007b. Reactivación de estructuras cretácicas durante la deformación miocena, faja plegada del Agrio, Neuquén. Revista de la Asociación Geológica Argentina 62(2), 299-307.

Zamora Valcarce, G., Zapata, T., Ramos, V.A., Rodriguez, F., Bernanrdo, L.M. 2009. Evolución tectónica del frente andino en Neuquén. Revista de la Asociación Geológica Argentina 65, 192–203.

Zapata, T., Brissón, I., Dzelalija, F. 1999. The role of basement in the Andean fold and thrust belt of the Neuquén Basin. In: Proceedings Thrust Tectonics, pp. 122–124, London.

Zapata, T.R., Córsico, S., Dzelalija, F., Zamora Valcarce, G. 2002. La faja plegada y corrida del Agrio: Análisis estructural y su relación con los estratos terciarios de la cuenca neuquina, Argentina. 5º Congreso de Exploración y Desarrollo de Hidrocarburos (Mar del Plata), Actas digitales.

Zollner, W., Amos, A.J. 1973. Descripción geológica de la Hoja 32b, Chos Malal (Prov. Neuquén). Servicio Geológico y Minero Argentino, Boletín 143, 1-91, Buenos Aires.

Figure Captions

Figure 1: Location and tectonic setting of the study area

Figure 2: Geological map of the study area. Structural cross sections are indicated with black lines, and the location of the samples used for fission track analyses with points. Red points indicate samples used for the thermal history model.

Figure 3: Regional structural cross section at 38º S. Note that the study area is located over the Agrio and Chos Malal fold and thrust belts where the maximum Mesozoic thickness occurs (modified from Rojas Vera et al., 2014).

Table 1 : Samples used for the apatite fission track analysis.

Figure 4: Structural cross sections across the Agrio, Chos Malal and Malargüe fold and thrust belts (modified from Zapata et al. 1999; Zamora Valcarce et al. 2007a).

Figure 5: Northern structural cross section and corresponding restoration. Note the presence of a basement block at the inner part, while to the east the Malargüe fold and thrust belt forms a triangle zone at the orogenic front.

Figure 6: Naunauco-Loma Rayoso central structural cross section and corresponding restoration. Note the presence of a basement block at the westernmost part, while to the east of the Agrio fold and thrust belt a triangle zone is developed. At these latitudes the orogenic front is characterized by the presence of basement structures forming the Chihuidos High. (Modified from Zamora Valcarce et al. 2007a).

Figure 7: Southern structural cross section and corresponding restoration. Again the inner part is characterized by a basement block, and the orogenic front is developed over basement structures corresponding to the Chihuidos High structure (Modified from Zapata et al. 1999; Zamora Valcarce et al. 2007a).

Figure 8: Thermal history model obtained for the samples located at the inner part of the Agrio and Chos Malal fold and thrust belts. These results were obtaining using the Hefty software.

Table 2: Fission track ages.

Figure 9: Thermal history model obtained for the samples located at the inner part of the Agrio and Chos Malal fold and thrust belt. These results were obtaining using the Hefty software.

Figure 10: Late Cretaceous- Paleocene exhumation. The orogenic front is highlighted with a red line.

Figure 11: Structural evolution of the northern section.

Figure 12: Structural evolution of northern section.

Figure 13: Structural evolution of southern section.

Sample Name	Unit	Age	Latitude	Longitude	Elevation
GC1132-1	Mulichinco Formation	Valanginian	-37.32	-70.03	1560
GC1132-2	Neuquén Group	Turonian	-37.64	-69.74	1167
GC1132-3	Agrio Formation	Hauterivian	-37.53	-70.00	1058
GC1132-4	Malargüe Group	Campanian-Maastrichtian	-37.61	-69.95	854
GC1132-5	Mulichinco Formation	Valanginian	-37.69	-70.52	1311
GC1132-6	Neuquén Group	Cenomanian	-37.85	-69.67	1347
GC1132-7	Mulichinco Formation	Valanginian	-37.99	-70.24	1065
GC1132-8	Tordillo Formation	Kimmeridgian	-38.02	-70.47	1268
GC1132-10	Lajas Formation	Bajocian	-37.97	-70.56	1124

Table 1 : Samples used for the apatite fission track analysis.

Sample	Number of crystals	N_s	N_i	N_D	ρ_s	ρ_i	ρ_D	χ^2	$P(\chi^2)$	U (ppm)	Central age (Ma±1σ)	Mean track length (μm)	Standard deviation (μm)	Number of tracks measured
GC1132-1	19	93	1022	2130	2.815E+05	3.093E+06	1.442E+06	44.081	0.1	24.5	23.6±4.5	12.95±0.28	1.89	47
GC1132-2	19	277	791	2130	3.599E+05	1.028E+06	1.427E+06	62.953	0.0	8.2	87.4±11.5	13.23±0.20	1.42	52
GC1132-3	19	259	3622	2130	2.913E+05	4.073E+06	1.412E+06	87.750	0.0	32.9	20.6±3.0	12.27±0.32	2.53	63
GC1132-4	19	286	1115	2130	3.607E+05	1.406E+06	1.398E+06	57.509	0.0	11.5	77.0±8.5	13.32±0.21	1.72	65
GC1132-5	19	538	3159	2130	5.116E+05	3.004E+06	1.383E+06	16.334	63.5	24.8	44.6±2.4	12.62±0.15	1.52	100
GC1132-6	20	627	2385	2130	1.052E+06	4.002E+06	1.369E+06	123.654	0.0	33.3	68.4±9.0	11.66±0.21	2.10	101
GC1132-7	19	328	2719	2130	3.991E+05	3.308E+06	1.354E+06	46.503	0.0	27.9	33.0±3.2	12.31±0.28	1.81	42
GC1132-8	9	139	668	2130	6.734E+05	3.236E+06	1.339E+06	10.736	29.4	27.5	52.9±5.2	12.62±0.67	2.02	9
GC1132-10	19	185	1133	2130	4.254E+06	2.606E+05	1.310E+06	28.517	7.4	22.7	43.6±4.9	13.61±0.25	1.14	21

All analyses carried out by C. Obrien (Geotrack Inc.). Ages calculated using a zeta value of 380.4±5.7 and CN5 dosimeter glass.
N_s = number of spontaneous tracks counted
N_i = number of induced tracks counted
N_D = number of tracks counted in dosimeter glass
ρ_s = density of spontaneous tracks
ρ_i = density of induced tracks
ρ_D = density of tracks in dosimeter glass
χ^2, $P(\chi^2)$ = chi-square statistics. A sample fails the chi-square test when $P(\chi^2)<5$.
U (ppm) = Uranium content calculated as (U content of standard glass * $\rho i/\rho D$)

Table 2: Fission track ages.

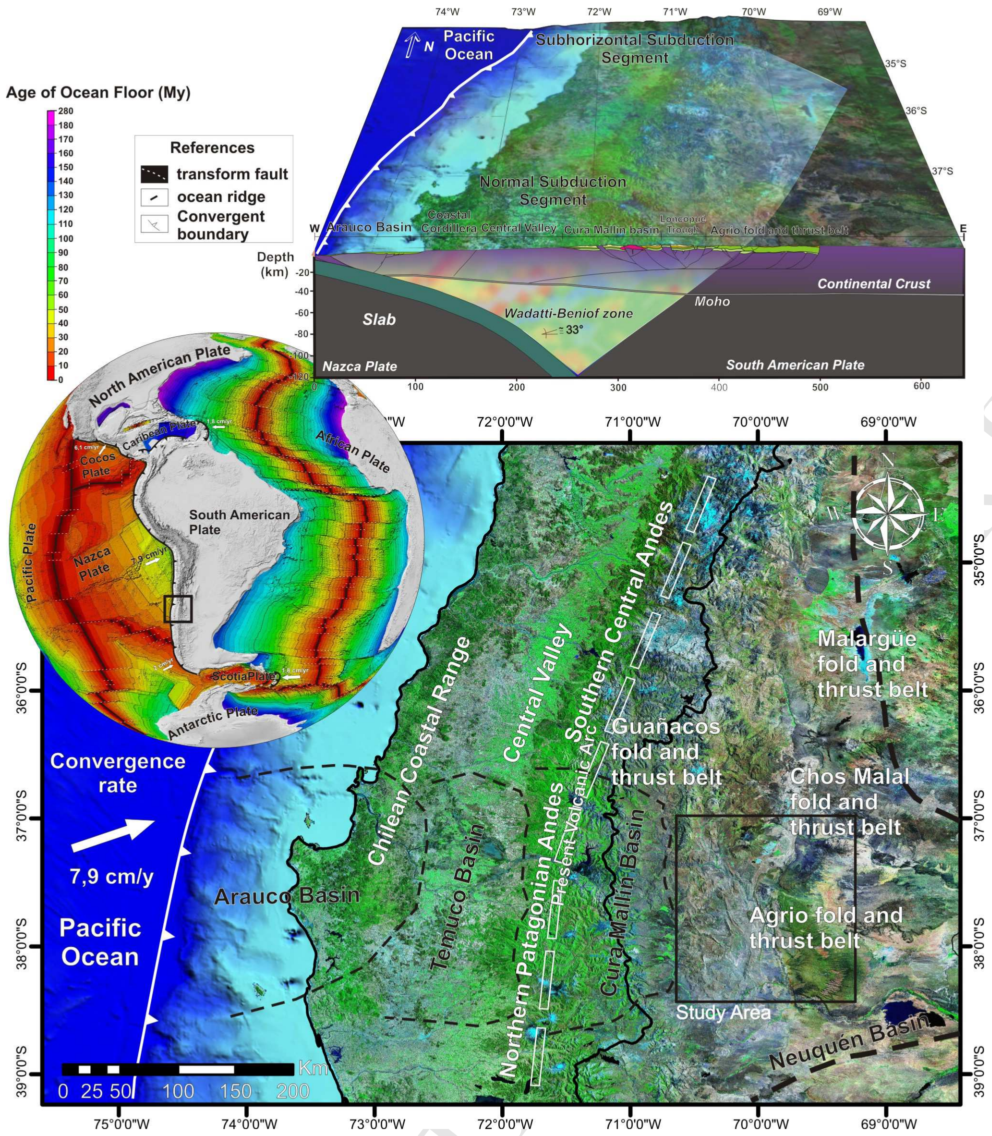
Age of Ocean Floor (My)
280
180
170
160
150
140
130
120
110
100
90
80
70
60
50
40
30
20
10
0
References
transform fault
ocean ridge
Convergent boundary
74°W
73°W
72°W
71°W
70°W
69°W
N
Pacific Ocean
Subhorizontal Subduction Segment
35°S
36°S
37°S
Normal Subduction Segment
W
Arauco Basin
Coastal Cordillera
Central Valley
Cura Mallin basin
Loncopué Trough
Agrio fold and thrust belt
E
Depth (km)
-20
-40
-60
-80
-100
-120
Continental Crust
Moho
Slab
Wadatti-Beniof zone
≅ 33°
Nazca Plate
South American Plate
0
100
200
300
400
500
600
North American Plate
Caribean Plate
Cocos Plate
African Plate
South American Plate
Pacific Plate
Nazca Plate
7,9 cm/yr
Scotia Plate
Antarctic Plate
72°0'0"W
71°0'0"W
70°0'0"W
69°0'0"W
35°0'0"S
36°0'0"S
37°0'0"S
38°0'0"S
39°0'0"S
Southern Central Andes
Malargue fold and thrust belt
Chilean Coastal Range
Central Valley
Guanacos fold and thrust belt
Chos Malal fold and thrust belt
Convergence rate
7,9 cm/y
Temuco Basin
Present Volcanic Arc
Northern Patagonian Andes
Cura Mallin Basin
Arauco Basin
Agrio fold and thrust belt
Pacific Ocean
Study Area
Neuquén Basin
0 25 50 100 150 200 Km
75°0'0"W
74°0'0"W
73°0'0"W

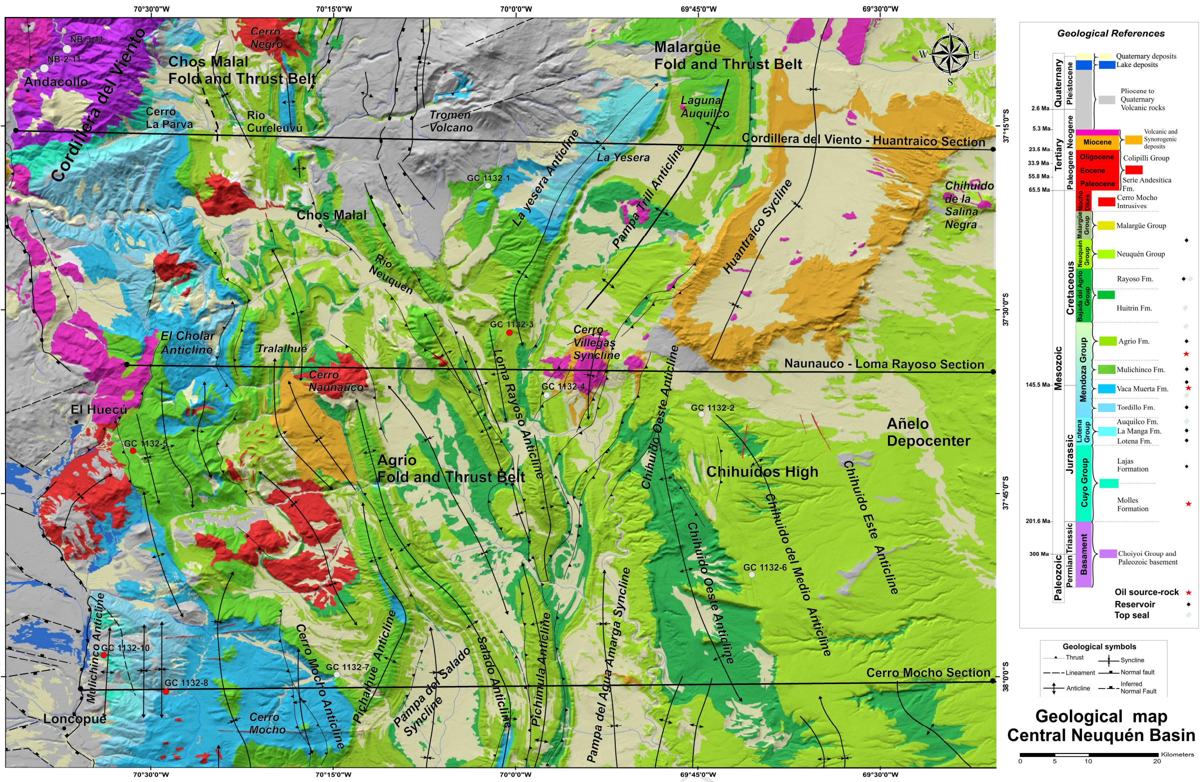
70°30'0"W
70°15'0"W
70°0'0"W
69°45'0"W
69°30'0"W
37°15'0"S
37°30'0"S
37°45'0"S
38°0'0"S
NB-2-12
NB-2-11
Andacollo
Cordillera del Viento
Chos Malal Fold and Thrust Belt
Cerro Negro
Cerro La Parva
Rio Cureleuvú
Tromen Volcano
Malargüe Fold and Thrust Belt
Laguna Auquilco
Cordillera del Viento - Huantraico Section
La Yesera
La Yesera Anticline
Pampa Trill Anticline
GC 1132-1
Chos Malal
Rio Neuquen
Huantraico Sycline
Chihuido de la Salina Negra
El Cholar Anticline
Tralalhué
GC 1132-3
Cerro Villegas Syncline
Cerro Naunauco
GC 1132-4
Naunauco - Loma Rayoso Section
El Huecú
GC 1132-5
GC 1132-2
Loma Rayoso Anticline
Chihuido Oeste Anticline
Añelo Depocenter
Agrio Fold and Thrust Belt
Chihuidos High
Chihuido Este Anticline
Chihuido del Medio Anticline
GC 1132-6
Chihuido Oeste Anticline
Mulichinco Anticline
GC 1132-10
GC 1132-8
Cerro Mocho Anticline
GC 1132-7
Pichaihue Anticline
Pampa del Salado Syncline
Salado Anticline
Pichimula Anticline
Pampa del Agua Amarga Syncline
Cerro Mocho Section
Loncopué
Cerro Mocho
N
E
S
W
Geological References
Quaternary
Pleistocene
Tertiary
Paleogene
Neogene
Miocene
Oligocene
Eocene
Paleocene
Mesozoic
Cretaceous
Jurassic
Paleozoic
Permian
Triassic
2.6 Ma
5.3 Ma
23.5 Ma
33.9 Ma
55.8 Ma
65.5 Ma
145.5 Ma
201.6 Ma
300 Ma
Quaternary deposits
Lake deposits
Pliocene to Quaternary Volcanic rocks
Volcanic and Synorogenic deposits
Colipilli Group
Serie Andesítica Fm.
Mocho Dikes
Cerro Mocho Intrusives
Malargüe Group
Neuquén Group
Bajada del Agrio Group
Rayoso Fm.
Huitrin Fm.
Mendoza Group
Agrio Fm.
Mulichinco Fm.
Vaca Muerta Fm.
Tordillo Fm.
Lotena Group
Auquilco Fm.
La Manga Fm.
Lotena Fm.
Cuyo Group
Lajas Formation
Molles Formation
Basament
Choiyoi Group and Paleozoic basement
Oil source-rock ★
Reservoir ◆
Top seal ✧
Geological symbols
Thrust
Syncline
Lineament
Normal fault
Anticline
Inferred Normal Fault
Geological map Central Neuquén Basin
0 5 10 20 Kilometers

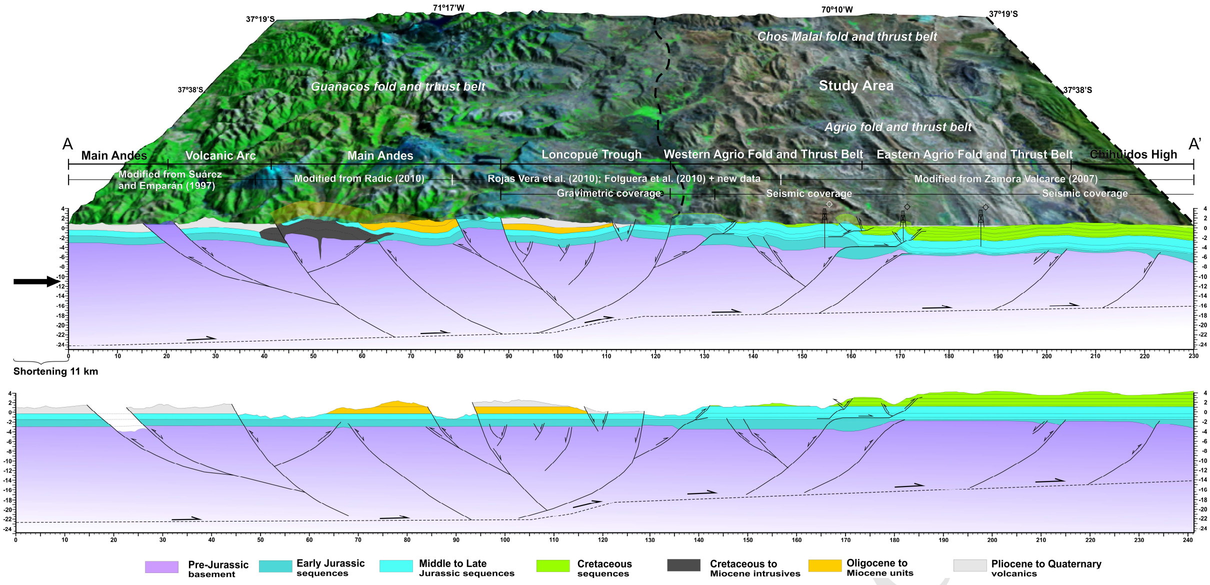
37º19'S
71º17'W
70º10'W
37º19'S
37º38'S
37º38'S
Chos Malal fold and thrust belt
Guañacos fold and trhust belt
Study Area
Agrio fold and thrust belt
A
A'
Main Andes
Volcanic Arc
Main Andes
Loncopué Trough
Western Agrio Fold and Thrust Belt
Eastern Agrio Fold and Thrust Belt
Chihuidos High
Modified from Suárez and Emparán (1997)
Modified from Radic (2010)
Rojas Vera et al. (2010); Folguera et al. (2010) + new data
Modified from Zamora Valcarce (2007)
Gravimetric coverage
Seismic coverage
Seismic coverage
4
2
0
-2
-4
-6
-8
-10
-12
-14
-16
-18
-20
-22
-24
0
10
20
30
40
50
60
70
80
90
100
110
120
130
140
150
160
170
180
190
200
210
220
230
240
Shortening 11 km
Pre-Jurassic basement
Early Jurassic sequences
Middle to Late Jurassic sequences
Cretaceous sequences
Cretaceous to Miocene intrusives
Oligocene to Miocene units
Pliocene to Quaternary volcanics

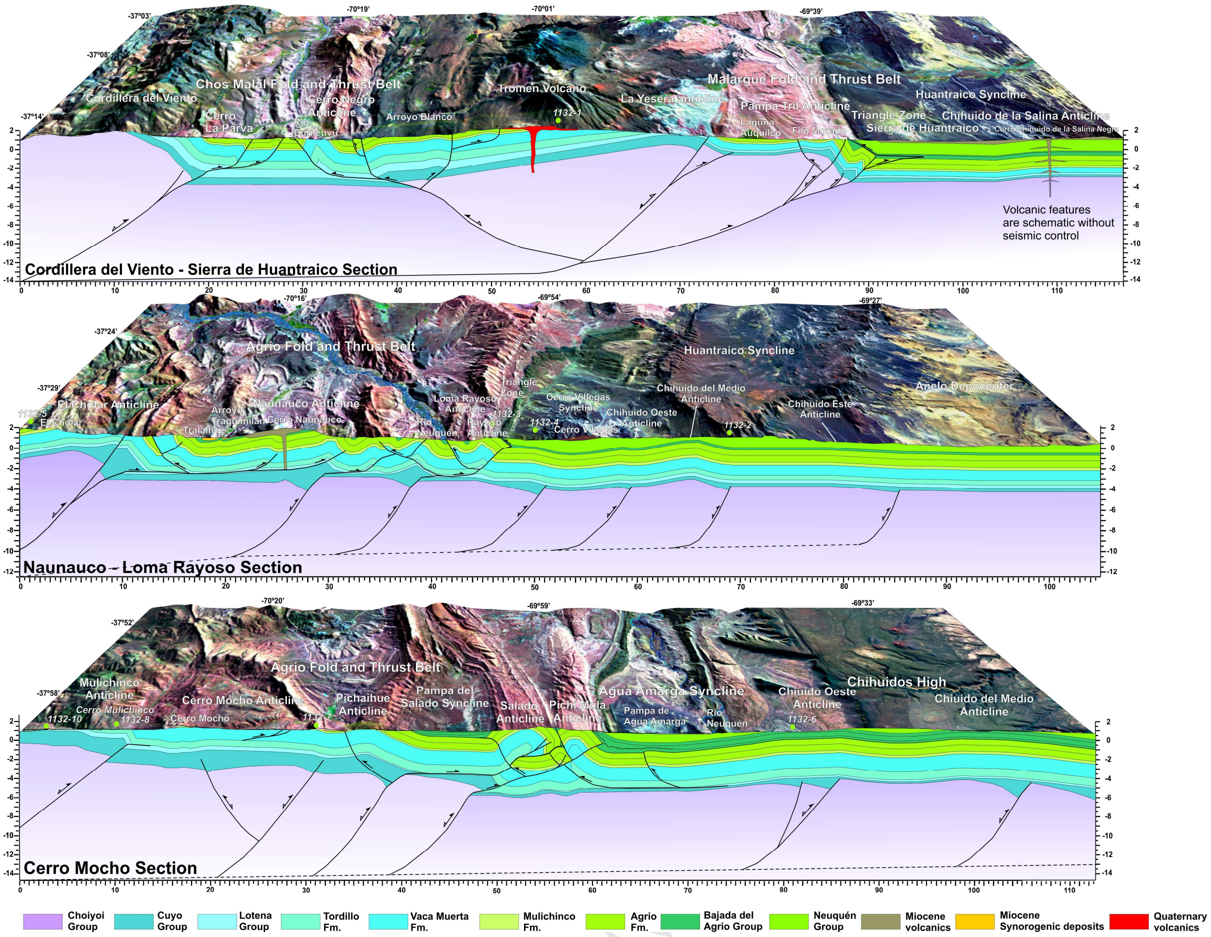
-37º03'
-37º08'
-37º14'
-70º19'
-70º01'
-69º39'
Chos Malal Fold and Thrust Belt
Cordillera del Viento
Cerro La Parva
Río Curileuvú
Cerro Negro Anticline
Arroyo Blanco
Tromen Volcano
1132-1
La Yesera anticline
Malargüe Fold and Thrust Belt
Pampa Tril Anticline
Laguna Auquilco
Filo Morado
Huantraico Syncline
Triangle Zone
Sierra de Huantraico
Chihuido de la Salina Anticline
Cerro Chihuido de la Salina Negra
Volcanic features are schematic without seismic control
Cordillera del Viento - Sierra de Huantraico Section
-70º16'
-69º54'
-69º27'
-37º24'
-37º29'
Agrio Fold and Thrust Belt
El Cholar Anticline
1132-5
El Cholar
Arroyo Traquimilan
Tralalhué
Naunauco Anticline
Cerro Naunauco
Río Neuquén
Loma Rayoso Anticline
Triangle Zone
1132-3
Rayoso Anticline
1132-4
Cerro Villegas Syncline
Cerro Villegas
Chihuido Oeste Anticline
Huantraico Syncline
Chihuido del Medio Anticline
1132-2
Chihuido Este Anticline
Añelo Depocenter
Naunauco - Loma Rayoso Section
-70º20'
-69º59'
-69º33'
-37º52'
-37º58'
Agrio Fold and Thrust Belt
Mulichinco Anticline
Cerro Mulichinco
1132-10
1132-8
Cerro Mocho Anticline
Cerro Mocho
1132-7
Pichaihue Anticline
Pampa del Salado Syncline
Arroyo Cauce Seco del Salado
Salado Anticline
Pichi Mula Anticline
Agua Amarga Syncline
Pampa de Agua Amarga
Río Neuquén
Chiuido Oeste Anticline
1132-6
Chihuidos High
Chiuido del Medio Anticline
Cerro Mocho Section
Choiyoi Group
Cuyo Group
Lotena Group
Tordillo Fm.
Vaca Muerta Fm.
Mulichinco Fm.
Agrio Fm.
Bajada del Agrio Group
Neuquén Group
Miocene volcanics
Miocene Synorogenic deposits
Quaternary volcanics

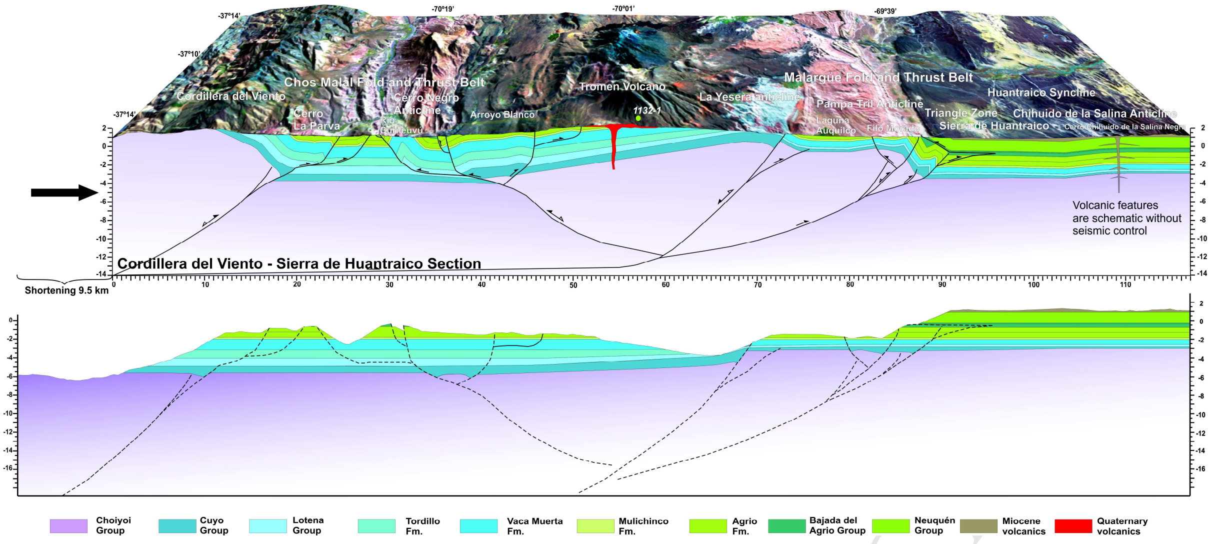
-37º14'
-37º10'
-37º14'
-70º19'
-70º01'
-69º39'
Chos Malal Fold and Thrust Belt
Cordillera del Viento
Cerro La Parva
Río Curileuvú
Cerro Negro Anticline
Arroyo Blanco
Tromen Volcano
1132-1
La Yesera anticline
Malargüe Fold and Thrust Belt
Pampa Tril Anticline
Laguna Auquilco
Filo Morado
Triangle Zone
Sierra de Huantraico
Huantraico Syncline
Chihuido de la Salina Anticline
Cerro Chihuido de la Salina Negra
Volcanic features are schematic without seismic control
Cordillera del Viento - Sierra de Huantraico Section
Shortening 9.5 km
0
10
20
30
40
50
60
70
80
90
100
110
2
0
-2
-4
-6
-8
-10
-12
-14
-16
Choiyoi Group
Cuyo Group
Lotena Group
Tordillo Fm.
Vaca Muerta Fm.
Mulichinco Fm.
Agrio Fm.
Bajada del Agrio Group
Neuquén Group
Miocene volcanics
Quaternary volcanics

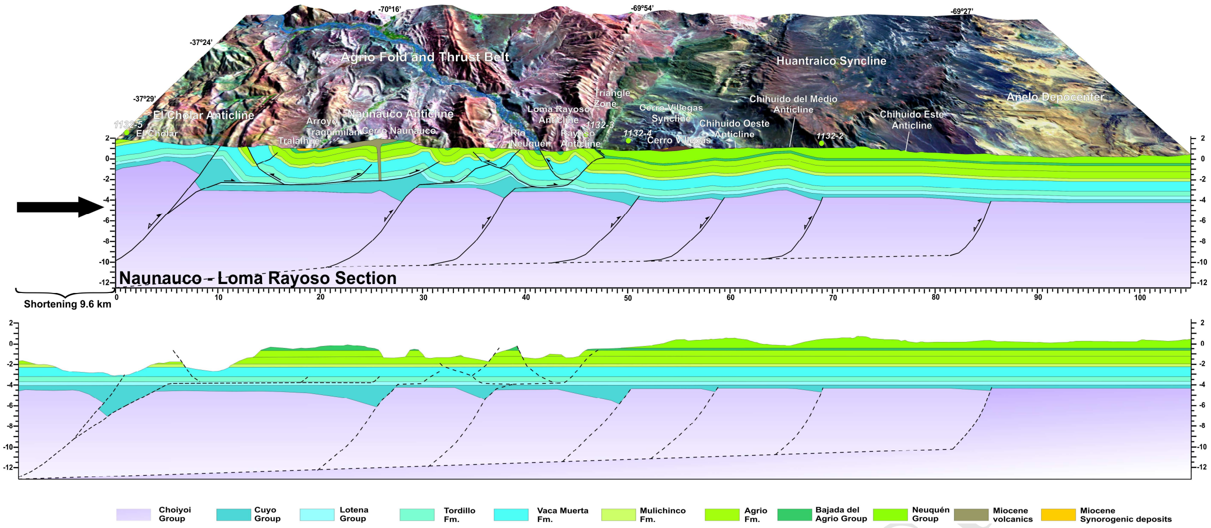
-70º16'
-69º54'
-69º27'
-37º24'
-37º29'
Agrio Fold and Thrust Belt
Huantraico Syncline
Añelo Depocenter
El Cholar Anticline
1132-5
El Cholar
Arroyo Traquimilan
Naunauco Anticline
Cerro Naunauco
Tralalhué
Loma Rayoso Anticline
Triangle Zone
1132-3
Río Neuquén
Rayoso Anticline
1132-4
Cerro Villegas Syncline
Cerro Villegas
Chihuido Oeste Anticline
Chihuido del Medio Anticline
1132-2
Chihuido Este Anticline
Naunauco - Loma Rayoso Section
Shortening 9.6 km
2
0
-2
-4
-6
-8
-10
-12
0
10
20
30
40
50
60
70
80
90
100
Choiyoi Group
Cuyo Group
Lotena Group
Tordillo Fm.
Vaca Muerta Fm.
Mulichinco Fm.
Agrio Fm.
Bajada del Agrio Group
Neuquén Group
Miocene volcanics
Miocene Synorogenic deposits

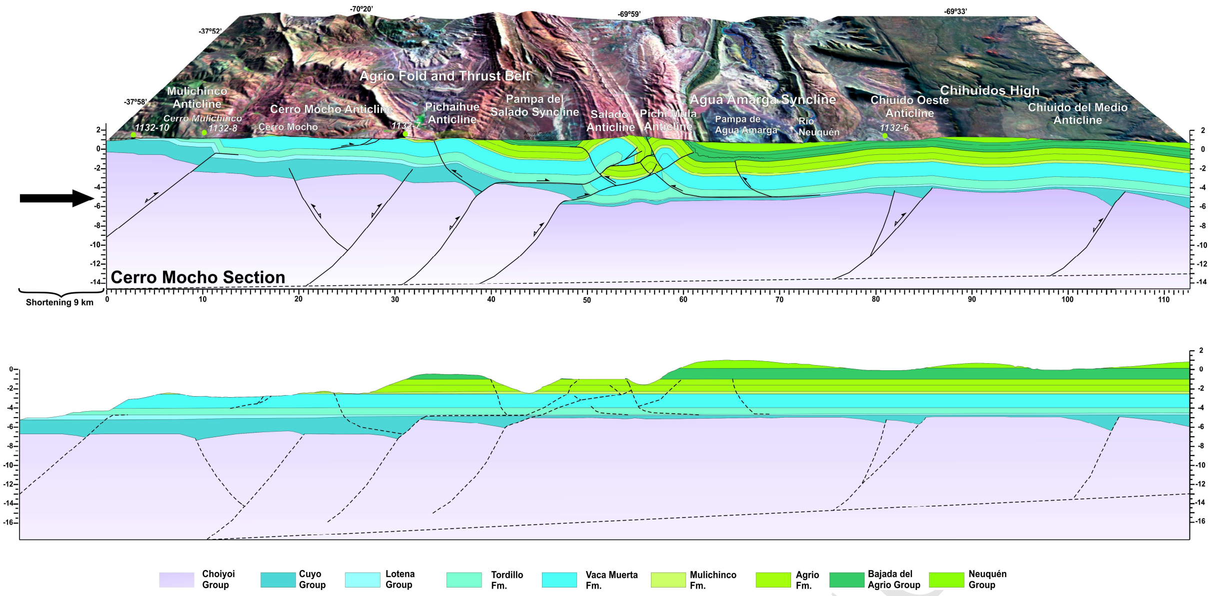
-70°20'
-69°59'
-69°33'
-37°52'
-37°58'
Agrio Fold and Thrust Belt
Mulichinco Anticline
Cerro Mulichinco
1132-10
1132-8
Cerro Mocho Anticline
Cerro Mocho
1132-7
Pichaihue Anticline
Pampa del Salado Syncline
Arroyo Cauce Seco del Salado
Salado Anticline
Pichi Mula Anticline
Agua Amarga Syncline
Pampa de Agua Amarga
Río Neuquén
Chiuido Oeste Anticline
1132-6
Chihuidos High
Chiuido del Medio Anticline
Cerro Mocho Section
Shortening 9 km
0
10
20
30
40
50
60
70
80
90
100
110
2
0
-2
-4
-6
-8
-10
-12
-14
-16
Choiyoi Group
Cuyo Group
Lotena Group
Tordillo Fm.
Vaca Muerta Fm.
Mulichinco Fm.
Agrio Fm.
Bajada del Agrio Group
Neuquén Group

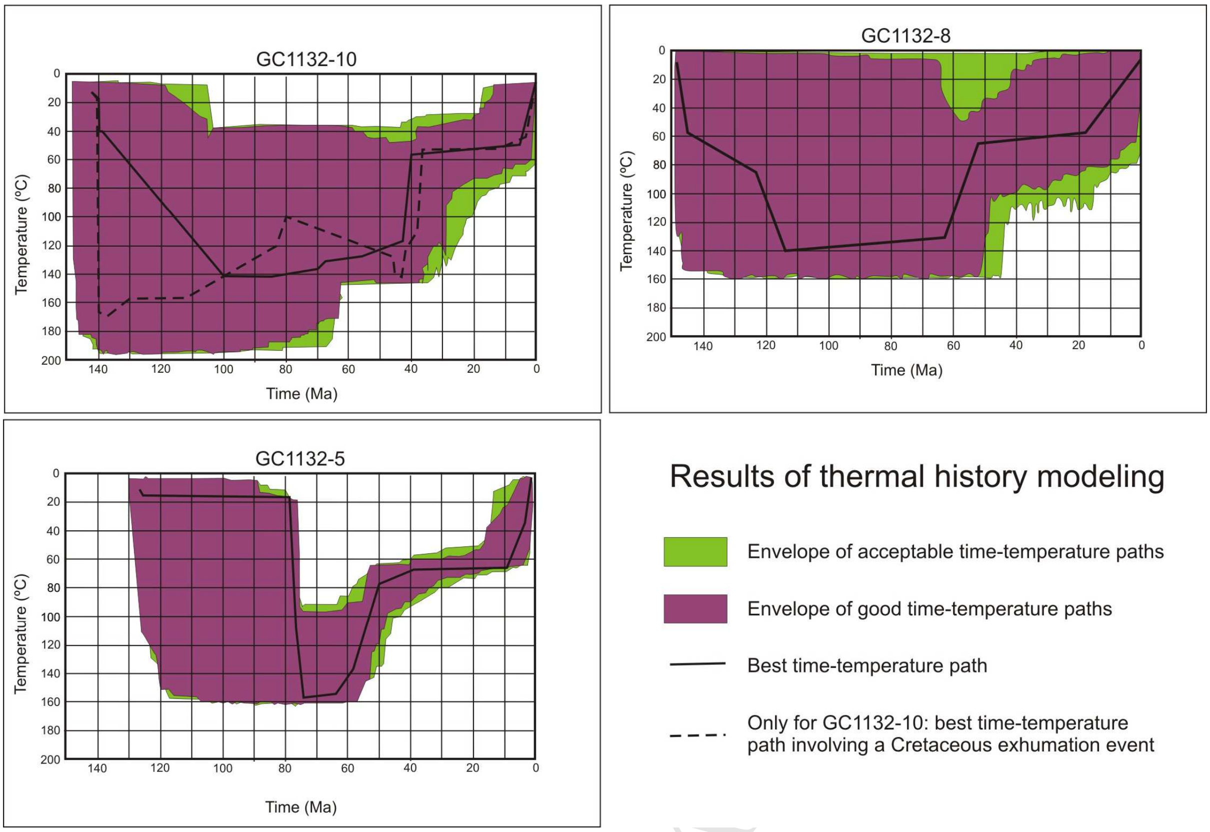
GC1132-10
GC1132-8
GC1132-5
Temperature (ºC)
Time (Ma)
0
20
40
60
80
100
120
140
160
180
200
140
120
100
80
60
40
20
0
Results of thermal history modeling
Envelope of acceptable time-temperature paths
Envelope of good time-temperature paths
Best time-temperature path
Only for GC1132-10: best time-temperature path involving a Cretaceous exhumation event

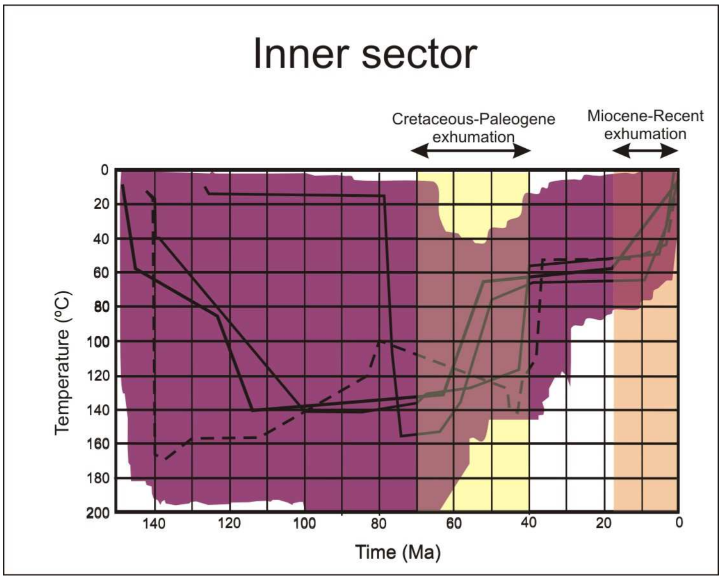
Inner sector
Cretaceous-Paleogene exhumation
Miocene-Recent exhumation
Temperature (ºC)
0
20
40
60
80
100
120
140
160
180
200
140
120
100
80
60
40
20
0
Time (Ma)

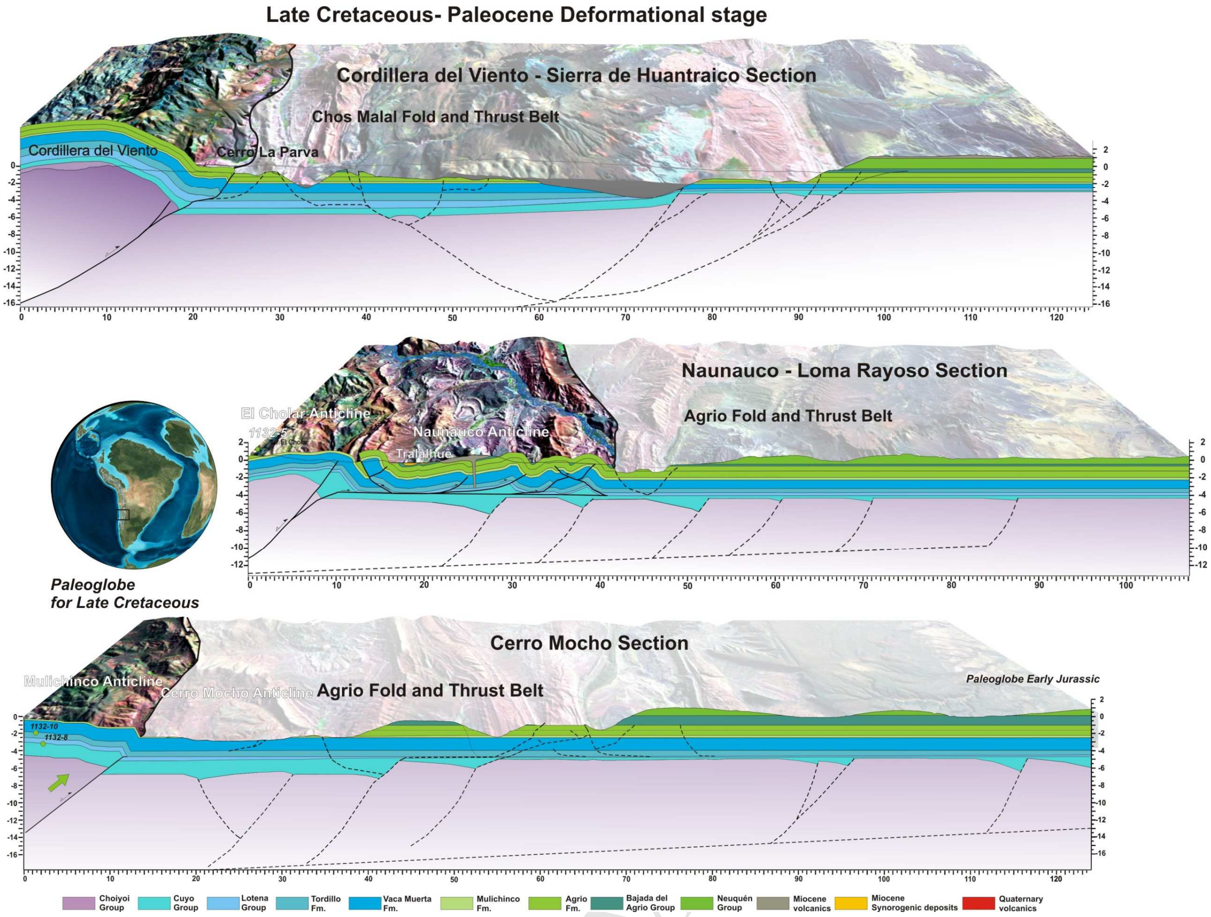
Late Cretaceous- Paleocene Deformational stage
Cordillera del Viento - Sierra de Huantraico Section
Chos Malal Fold and Thrust Belt
Cordillera del Viento
Cerro La Parva
Naunauco - Loma Rayoso Section
Agrio Fold and Thrust Belt
El Cholar Anticline
1132-5
El Cholar
Naunauco Anticline
Tralalhué
Paleoglobe
for Late Cretaceous
Cerro Mocho Section
Mulichinco Anticline
Cerro Mocho Anticline
Agrio Fold and Thrust Belt
Paleoglobe Early Jurassic
1132-10
1132-8
Choiyoi Group
Cuyo Group
Lotena Group
Tordillo Fm.
Vaca Muerta Fm.
Mulichinco Fm.
Agrio Fm.
Bajada del Agrio Group
Neuquén Group
Miocene volcanics
Miocene Synorogenic deposits
Quaternary volcanics

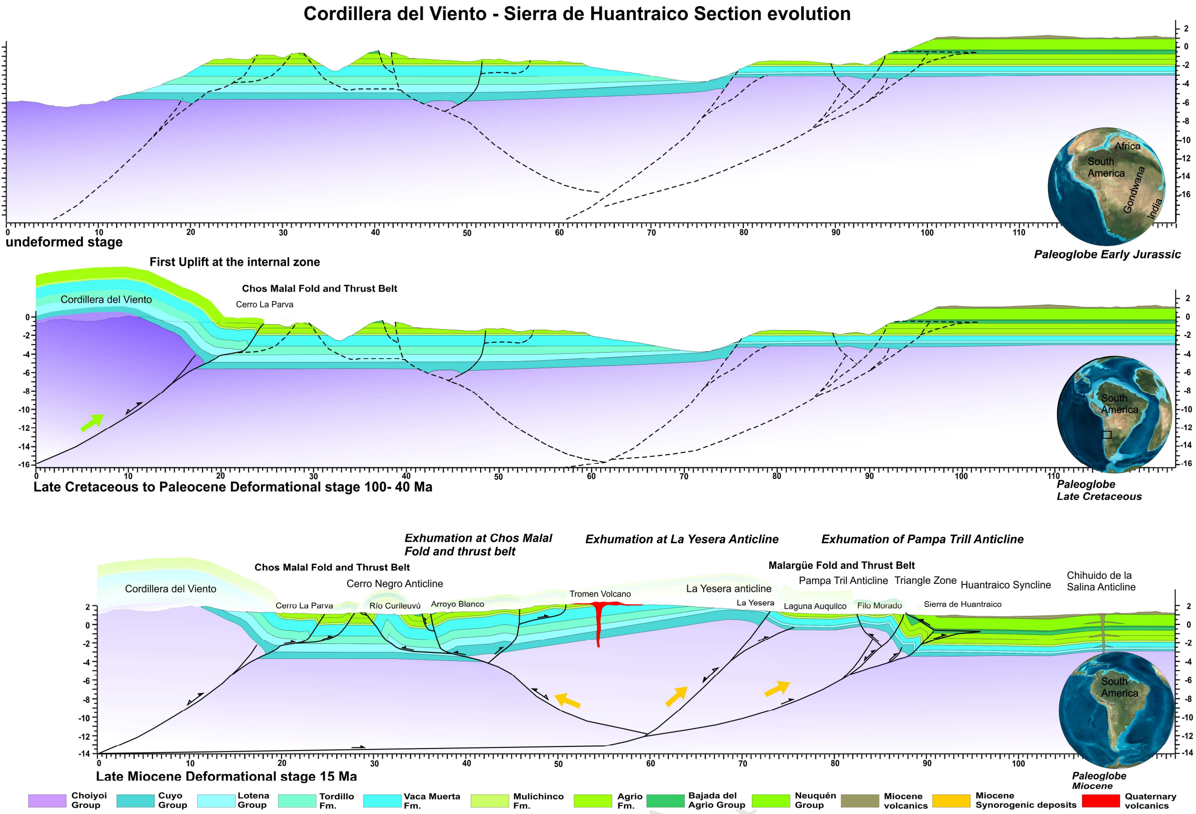
Cordillera del Viento - Sierra de Huantraico Section evolution
undeformed stage
Paleoglobe Early Jurassic
Africa
South America
Gondwana
India
First Uplift at the internal zone
Cordillera del Viento
Chos Malal Fold and Thrust Belt
Cerro La Parva
Late Cretaceous to Paleocene Deformational stage 100- 40 Ma
South America
Paleoglobe Late Cretaceous
Exhumation at Chos Malal Fold and thrust belt
Exhumation at La Yesera Anticline
Exhumation of Pampa Trill Anticline
Cordillera del Viento
Chos Malal Fold and Thrust Belt
Cerro Negro Anticline
Cerro La Parva
Rio Curileuvú
Arroyo Blanco
Tromen Volcano
La Yesera anticline
La Yesera
Malargüe Fold and Thrust Belt
Pampa Tril Anticline
Laguna Auquilco
Triangle Zone
Filo Morado
Huantraico Syncline
Sierra de Huantraico
Chihuido de la Salina Anticline
South America
Late Miocene Deformational stage 15 Ma
Paleoglobe Miocene
Choiyoi Group
Cuyo Group
Lotena Group
Tordillo Fm.
Vaca Muerta Fm.
Mulichinco Fm.
Agrio Fm.
Bajada del Agrio Group
Neuquén Group
Miocene volcanics
Miocene Synorogenic deposits
Quaternary volcanics

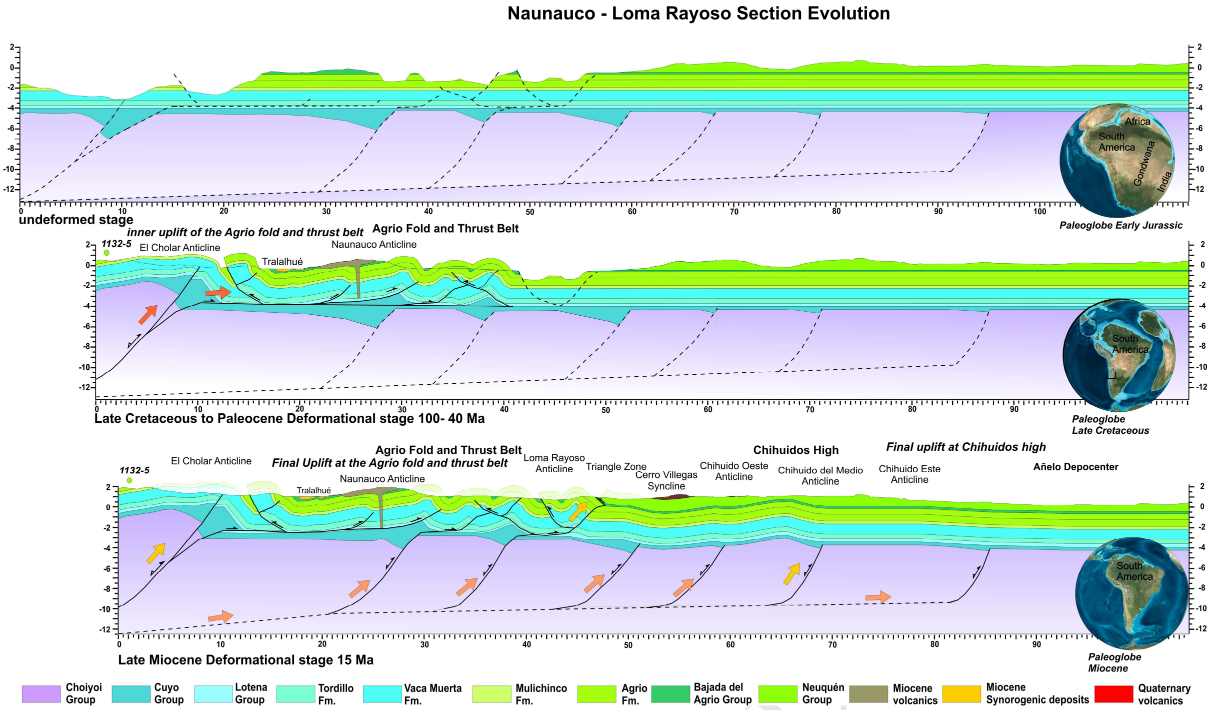
Naunauco - Loma Rayoso Section Evolution
undeformed stage
Paleoglobe Early Jurassic
Africa
South America
Gondwana
India
inner uplift of the Agrio fold and thrust belt
Agrio Fold and Thrust Belt
1132-5
El Cholar Anticline
Naunauco Anticline
Tralalhué
Late Cretaceous to Paleocene Deformational stage 100- 40 Ma
Paleoglobe Late Cretaceous
South America
Agrio Fold and Thrust Belt
Final Uplift at the Agrio fold and thrust belt
1132-5
El Cholar Anticline
Tralalhué
Naunauco Anticline
Loma Rayoso Anticline
Triangle Zone
Cerro Villegas Syncline
Chihuido Oeste Anticline
Chihuidos High
Chihuido del Medio Anticline
Final uplift at Chihuidos high
Chihuido Este Anticline
Añelo Depocenter
Late Miocene Deformational stage 15 Ma
Paleoglobe Miocene
South America
2
0
-2
-4
-6
-8
-10
-12
0
10
20
30
40
50
60
70
80
90
100
Choiyoi Group
Cuyo Group
Lotena Group
Tordillo Fm.
Vaca Muerta Fm.
Mulichinco Fm.
Agrio Fm.
Bajada del Agrio Group
Neuquén Group
Miocene volcanics
Miocene Synorogenic deposits
Quaternary volcanics

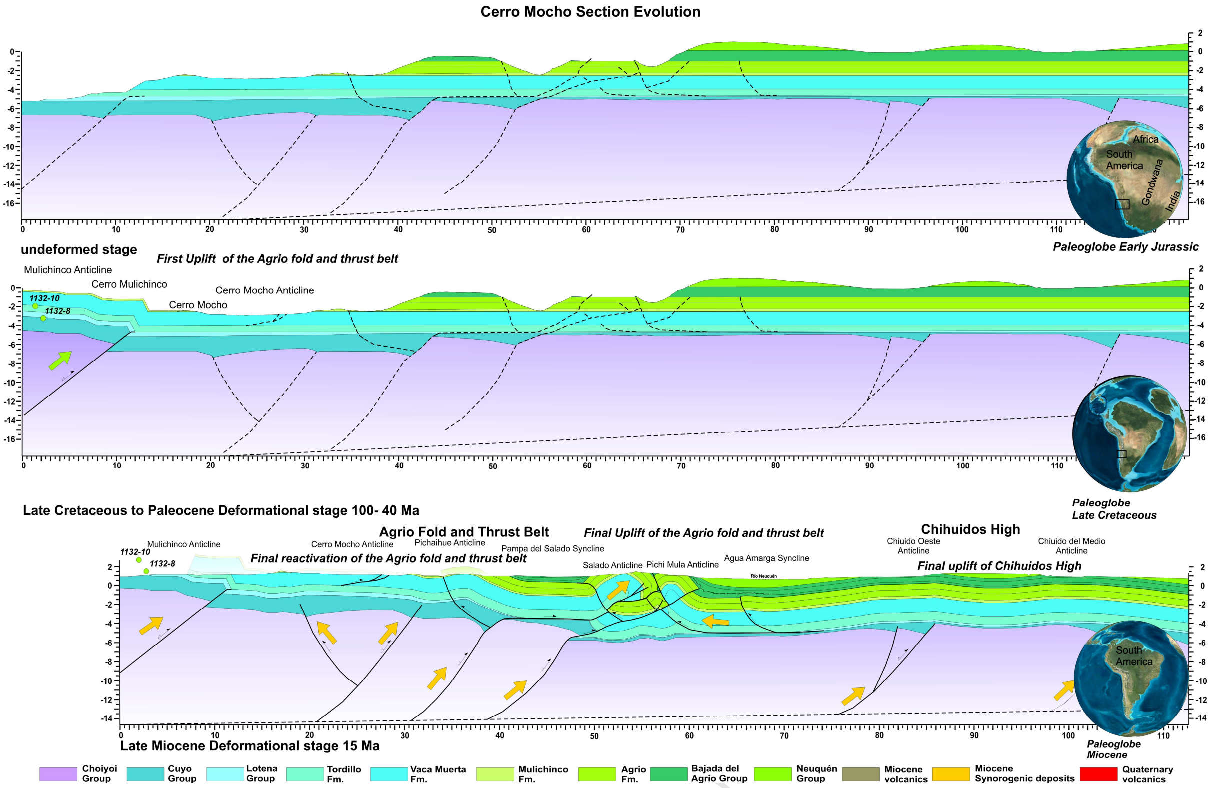
Cerro Mocho Section Evolution
undeformed stage
Paleoglobe Early Jurassic
Africa
South America
Gondwana
India
First Uplift of the Agrio fold and thrust belt
Mulichinco Anticline
Cerro Mulichinco
Cerro Mocho Anticline
Cerro Mocho
1132-10
1132-8
Late Cretaceous to Paleocene Deformational stage 100- 40 Ma
Paleoglobe Late Cretaceous
Agrio Fold and Thrust Belt
Final Uplift of the Agrio fold and thrust belt
Chihuidos High
Mulichinco Anticline
Cerro Mocho Anticline
Pichaihue Anticline
Pampa del Salado Syncline
Final reactivation of the Agrio fold and thrust belt
Salado Anticline
Pichi Mula Anticline
Agua Amarga Syncline
Río Neuquén
Chiuido Oeste Anticline
Chiuido del Medio Anticline
Final uplift of Chihuidos High
South America
Late Miocene Deformational stage 15 Ma
Paleoglobe Miocene
2 0 -2 -4 -6 -8 -10 -12 -14 -16
0 10 20 30 40 50 60 70 80 90 100 110
Choiyoi Group
Cuyo Group
Lotena Group
Tordillo Fm.
Vaca Muerta Fm.
Mulichinco Fm.
Agrio Fm.
Bajada del Agrio Group
Neuquén Group
Miocene volcanics
Miocene Synorogenic deposits
Quaternary volcanics

We construct regional structural cross sections for the Agrio and Chos Malal fold and thrust belts, based on field, seismic and well data.

FissION track dating was performed over the cross sections

This part of the Andes was structured through two compressional stages

A Late Cretaceous to Paleocene was the responsible to the first deformational event

A Late Miocene is the final stage that shaped these fold and thrust belts